Macroecological predictions of global biodiversity from remote sensing metrics

by

Marie-Bé Leduc

Thesis submitted to the Faculty of Graduate and Postdoctoral Studies, University of Ottawa, in partial fulfillment of the requirements for the M.Sc. Degree in the Ottawa-Carleton Institute of Biology, with specialization in Environmental Sustainability from the University of Ottawa Institute for the Environment.

Thèse soumise à la Faculté des études supérieures et postdoctorales, Université d'Ottawa en vue de l'obtention de la maîtrise en sciences de l'Institut de Biologie d'Ottawa-Carleton, avec spécialisation en durabilité environnementale de l'Institut de l'Environnement de l'Université d'Ottawa.

Acknowledgements

Thank you to NSERC and the Macroecology and Conservation lab for providing the funding to support my work, as well as the University of Ottawa for granting me with a scholarship and a work stipend for two years.

I am thankful to so many people who helped me complete this project, but first and foremost, to Jeremy Kerr for his generous support and encouragement, for inciting thoughtful discussions in the lab, for expecting the best from me, for enabling me to attend CSEE and Ecology Across Borders, for facilitating my involvement in policy projects and so much more! Thank you to the members of my committee, Dr. Anders Knudby and Dr. Joseph Bennett, along with Dr.Heather Kharouba, for their valuable comments and guidance. Thank you to the Shallow Water Earth Observation Lab, especially Anders Knudby for his invaluable GIS and remote sensing expertise, Matúš Hodúl for his advice with python, and Dr. Yongming Xu for his help while selecting and processing remote sensing datasets. From his undergraduate project supervision and biostatistics course, Dr. Antoine Morin has also been a very important part to the success of this project.

Throughout these two years, I had a great team to rely on. I thank the members of the Kerr lab – Peter, Catherine, Anouk, Tiffany, Paige, Courteney, Emily, Barbara, Rosie, Yulun – first of all for their critical input and technical assistance to my project, but also for their passion, their will to make a difference, and their readiness to make the most out of their time as early career scientists. They inspired me to make the most out of my time, and I had a great time working with them.

Many people have been important to the smooth progression of this thesis by providing the moral support to keep me going. Thank you to my parents – Sylvain and Marie-Claude – for *bee*ing attentive and loving, for encouraging me to be best that I can be, for translating and revising so many of my texts, and for expanding my collection of bee puns ;). My friends – Maude, Dom, Kayla, Stéphane, Amy, Sebastian, Phil, Isa – are inspirations in their own unique way and have brought me encouragement and good times throughout the process. Thank you to my partner Jake for being there and doing that all the time, for keeping me laughing, and for putting everything in perspective when things were difficult. Thank you to the Asian Climbing Club (ACC) for keeping me active and outside, and for providing some good friendly competition.

Finally, I thank the many people and groups – Saorla Kavanagh from Dublin City University, Let's Talk Science program, Planet Earth, Alex Honnold, Boris Peresechensky – that have been a great source of inspiration and who have, throughout the years, encouraged me dream big and have taught me the value of being perseverant.

Table of Contents

Abstract

Rapid biodiversity change at a global scale requires enhanced monitoring tools to predict how shifting environmental conditions might alter species' extinction risk. Emerging remote sensing tools are essential to these efforts and provide the sole mechanism to detect environmental changes and their potential consequences for biodiversity rapidly. Here, I assess the extent to which remote sensing measurements predict species richness globally and within regions, facilitating the establishment of a single framework for monitoring diversity worldwide. I assembled global remote sensing metrics and data on diversity gradients to construct and cross-validate models predicting species richness of birds and mammals within and among the world's biogeographic zones. Enhanced vegetation Index (EVI), land surface temperature (LST), the first principal component of habitat heterogeneity, and an interaction between energy and habitat heterogeneity are important remotely-sensed environmental measurements for predicting trends of species richness of birds and mammals at all scales, although the intensity of the relationship differs between groups and grain sizes. However, a global model does not explain differences in species richness of birds between distinct zoogeographical realms, indicating a possible threshold in biodiversity change prediction before onset of novel environmental conditions. Measuring potential nonlinear changes in species richness is a useful application of the essential biodiversity variables (EBV) framework for operational monitoring of global and regional biodiversity. The continued production of reliable and consistent remote sensing will facilitate further exploration of current and upcoming drivers of biodiversity change and will help improve macroecological models.

Résumé

Les changements rapides de la biodiversité à l'échelle planétaire requièrent de nouveaux outils de télédétection capables de détecter les changements environnementaux et les conséquences possibles de ces derniers sur la biodiversité et de prédire les risques d'extinction des espèces. Cette recherche évalue dans quelle mesure les données de télédétection peuvent effectivement prédire la diversité des espèces à l'échelle mondiale et à l'intérieur des régions, ceci dans le but de faciliter la mise en place d'un système de surveillance globale de la biodiversité. Nous avons rassemblé des mesures de télédétection et des données sur la biodiversité pour construire et valider des modèles prédictifs de la richesse des espèces, chez les oiseaux et les mammifères, à l'intérieur et entre les zones biogéographiques du monde. L'indice de végétation amélioré (EVI), la température de la surface terrestre (LST), la composante principale (PC) de l'hétérogénéité de l'habitat ainsi que l'interaction entre énergie et hétérogénéité de l'habitat sont des mesures importantes de télédétection bien que l'intensité de la relation diffère entre les groupes taxonomiques et la taille des quadrats. Par contre, un modèle global est insuffisant pour expliquer les différences dans la richesse des espèces selon les différentes zones biogéographiques. Ceci pourrait indiquer un seuil au-delà duquel la capacité à prédire les changements de la biodiversité face à de nouvelles conditions environnementales est incertaine. Enfin, l'accumulation fiable de données de télédétection afin de d'explorer les causes des changements de la diversité biologique constitue une application utile des variables essentielles de la diversité (EBV) et contribuera à améliorer les modèles macroécologiques.

List of Tables

List of Figures

Macroecological predictions of global biodiversity from remote sensing metrics

Introduction

Biodiversity losses have accelerated globally as a result of human activities (Pimm et al., 2014). To address this challenge, it is important to know how many species are at risk of being lost, where changes are occurring, and the causes of extinction. The contribution of fundamental macroecological research has provided a better understanding of the key processes governing where species are found and why species ranges change through time (Boucher-Lalonde, Kerr, & Currie, 2014; Currie et al., 2004; Lewthwaite, Debinski, & Kerr, 2016). Broad-scale approaches to predicting regional species numbers have proven highly successful, irrespective of taxon (Hawkins et al., 2003) or region (Jetz & Fine, 2012), and these predictions have proven robust through time also (Algar, Kharouba, Young, & Kerr, 2009; Fritz et al., 2016). Such models include mechanistic justifications that draw upon hypotheses related to climate, habitat extent, habitat heterogeneity, and historically contingent events, but rely on correlative tests for their support. Stronger tests of these patterns rely on experimentation or pseudo-experimental tests to determine whether observed relationships are consistent through time and might, as a consequence, be causal (Kerr, Kharouba, & Currie, 2007). Rapid change in climatic conditions and the landscape provides opportunities to test the strength of well-established species-environment associations (Algar et al., 2009; Kerr et al., 2007). Because there are significant regional differences in the relationships between environmental factors and gradients of species richness, environmental changes may

exceed historically observed conditions. Predictions of how biodiversity change may proceed seem likely to become less certain when conditions begin to exceed those upon which diversity-environmental relationships have been based within each region. Measuring those limits can inform the boundaries of potentially predictable biodiversity change and may consequently inform conservation decision-making.

Patterns of species richness across many taxa depend strongly on a few key environmental factors (Hawkins et al., 2003; Kalmar & Currie, 2007; Qian & Ricklefs, 2008). Climate and climate-related variables have historically gained the most support for their role in influencing geographic variations in species richness gradients (Currie, 1991; Field et al., 2009; Hawkins et al., 2003; Mittelbach et al., 2001). However, region-specific and evolutionary factors strongly affect gradients of species richness (Belmaker & Jetz, 2015; Qian, 2008, 2010), reducing the effectiveness of predictions that draw only on models linking environmental conditions to contemporary gradients of species richness. Moreover, present-day diversity trends may be much more closely related to human-related influences and climate variability than was true historically (Fritz et al., 2016). For instance, ongoing habitat loss and fragmentation have altered the distribution of birds and mammals in many regions of the world, and represent an impending threat to species persistence (Hof, Araújo, Jetz, & Rahbek, 2011; Mantyka-Pringle et al., 2015; Newbold, 2018). Changing temperatures, coupled with land use changes, are likely to increase extinction rates, thus altering local and broad-scale biodiversity dynamics (Mantyka-Pringle, Martin, & Rhodes, 2012; H. M. Pereira, Leadley, et al., 2010). Environmental changes that are consequent to human activities, as well as region-specific historical events, could modify expected relationships between widely acknowledged

predictors of species richness and diminish the chances that biodiversity change can be predicted successfully.

Taxonomic, temporal, and geographic biases in data availability limit assessments and predictions of biodiversity change regionally and globally (Pereira, Belnap, et al., 2010; Pereira, Navarro, & Martins, 2012; Proença et al., 2016). For example, the Living Planet Index is perhaps the largest time-series database of vertebrate populations but has many fewer observations in tropical environments compared with temperate environments (Butchart et al., 2010; Collen et al., 2009). Yet, to the extent that present-day environmental conditions determine gradients of species richness, predicting gradients of diversity and diversity change may nevertheless be possible. Using remote sensing information, Essential Biodiversity Variables (EBVs) are designed to reflect a wide array of factors that may affect the origins and persistence of gradients of diversity, facilitating the generation of a comprehensive monitoring network that could improve biodiversity assessments worldwide (Pereira et al., 2013).

Remote sensing provides unique capacities to measure environmental conditions across broad areas nearly in real-time, detecting even subtle changes in environmental factors that have been linked to species richness (Kerr & Ostrovsky, 2003; O'Connor et al., 2015; Pettorelli, Owen, & Duncan, 2016). Satellite remote sensing provides global coverage of the Earth's surface at high temporal and spatial resolutions. Such data are relatively easy to access and can be manipulated using GIS platforms to support conservation efforts and environmental management decision-making (Pettorelli, Safi, & Turner, 2014; Turner et al., 2015). More importantly, the long lifetime of satellite missions enables continuous observations over years or decades that can contribute

meaningfully to global biodiversity monitoring through integration within the EBV framework, especially when combining remotely-sensed and *in situ* data in modelling (Pettorelli, Wegmann, et al., 2016; Skidmore et al., 2015). As a result, satellite remote sensing EBVs (SR-RBVs) may play a critical role in advancing fundamental knowledge around the origins and maintenance of global gradients of biodiversity and deliver first-order estimates of the effects of changing environmental conditions on biodiversity gradients worldwide.

Here, I test the extent to which available remotely-sensed Essential Biodiversity Variables explain current global trends of biodiversity. Past and current models describing broad-scale biodiversity trends in relation to environmental conditions often use interpolated weather station data, which have much less capacity to be updated as changes happen. I gathered an array of remote sensing metrics and data on biodiversity gradients, to construct models predicting species richness of birds and terrestrial mammals globally. Secondly, I explore the potential and implications of using global and regional models to make predictions on biodiversity trends globally. Under new environmental circumstances, our capacity to predict biodiversity might be bounded by present-day conditions. Given these constraints, I assess potential environmental limits to prediction based on environment diversity relationships.

Methods

Study area and sampling system

Three grid systems of equal area quadrats (100km x 100 km, 200 x 200km, 400km x 400km)[1] were created over all continents except Antarctica using Goode Homolosine equal area projection. Antarctica was excluded from my study because most remote sensing datasets did not have information for this latitude. To account for the species-area relationship, which describes an increase in species richness with an increase in area (Connor & McCoy, 1979; Preston, 1962), quadrats for which land area was less than 50% of the total area were removed from the study (i.e. 5000km^2, 20 000km^2, and 80 000km^2). All geographic analysis were performed using ArcGIS 10.4, arcpy and python (*ESRI*, 2016).

Species data

Digital distribution maps for the 5271 species of terrestrial mammals used in this study were downloaded from The IUCN Red List of Threatened Species Spatial Data Download webpage (IUCN, 2016). The most recent version includes information on species ranges that have been updated over the 2008-2017 period. Although the dataset is missing information on some newly described species or species from poorly studied regions, the rate of new mammal species descriptions and mapping remains high.

Distribution maps for 10,838 species of birds were obtained from BirdLife International and Handbook of the Birds of the World (BirdLife International and Handbook of the Birds of the World, 2016). This includes specimen localities from BirdLife's Point Locality Database, the Global Biodiversity Information Facility (GBIF), observer records from BirdLife's International Red Data Books, published literature,

[1] See Appendix A, Figure A1, for maps of quadrat systems

survey reports, distribution atlases, field guides, expert opinion and other unpublished sources. Most recent updates range from 1998-2016.

Subspecies and subpopulations were merged as a single species, and all range maps were cropped to the extent of continental land masses. Species richness was calculated by summing the number of species maps on a per quadrat basis for each grid system[2].

Remote sensing data

Environmental variables were selected on the basis of their importance for explaining large-scale variations in species richness, as described in previous studies (Currie, 1991; Evans, James, & Gaston, 2006; Hawkins et al., 2003; Jetz & Fine, 2012; Rahbek et al., 2007; Whittaker, Nogués-Bravo, & Araújo, 2007), and their availability from remote sensing platforms. The annual mean, maximum, and minimum for continuous variables were obtained for each year between 2001-2010, and were averaged over this 10 year period, and spatially averaged for each grid system[3]. The spatial standard deviation was obtained as a measure of environmental heterogeneity. A total of 30 distinct variables were included (Table 1) and grouped according to well-established biological hypothesis found in macroecology and biogeography studies, including:

1 Productive energy, often measured as primary productivity, can increase species richness via several known mechanisms including elevating the number of individuals that a locality can support thus reducing extinction rates, increasing turnover and speciation rates, and reducing minimum viable population sizes (Evans et al., 2006; Evans, Warren, & Gaston, 2005; Honkanen, Roberge, Rajasärkkä, & Mönkkönen, 2010;

[2] See Appendix A, Figure A2, for species richness maps
[3] See Appendix A, Figure A3, A4, A5, for examples of remote sensing datasets

Wright, 1983). Measurements of productive energy include Net Primary Productivity (NPP) and Gross Primary Productivity (GPP) obtained through the Numerical Terradynamic Simulation Group (NTSG) (Running et al., 2004; Zhao, Heinsch, Nemani, & Running, 2005). I also included simpler measures of productivity, the normalized difference vegetation index (NDVI) and the enhanced vegetation index (EVI) (Didan, 2015), that have been used widely in the literature to monitor vegetation photosynthesis through time and space. NDVI and EVI were shown to relate strongly to net primary productivity and photosynthetic capacity in various environments (Coops, Waring, & Landsberg, 1998; Huete et al., 2002; Pettorelli et al., 2011). The Dynamic Habitat Index (DHI), based on the fraction of photosynthetically active radiation (fPAR), incorporates three components of vegetation light absorbance. The components are cumulative (DHI-cum), minimum (DHI-min) and the seasonal variation (DHI-var) in fPAR, which have been used to predict patterns of avian species richness (Coops, Waring, Wulder, Pidgeon, & Radeloff, 2009; Coops, Wulder, Duro, Han, & Berry, 2008).

2) Heat-related energy, via solar radiation, influences species richness through various mechanisms, including the creation of suitable climatic conditions and the regulation of speciation and extinction rates (Belmaker & Jetz, 2015; Currie, 1991; Currie et al., 2004; Evans et al., 2005). Measurements of ambient energy include monthly composited average of land surface temperature (LST) and potential evapotranspiration (PET) available from MODIS (Wan, Hook, & Hulley, 2015) and via the NTSG[4] (Mu, Zhao, & W Running, 2011).

[4] See Appendix A, Table A1, for the list of acronyms and abbreviations

3) Habitat heterogeneity defines broad-scale variation in species richness by moderating the effect of land use intensity (Gámez-Virués et al., 2015; Perović et al., 2015), expanding niche space and promoting species resilience and coexistence (Kadmon & Allouche, 2007; Laliberté & Tylianakis, 2010), and by providing opportunities for refuge and isolation (Fjeldså, Bowie, & Rahbek, 2012). I derived multiple remote sensing metrics capturing different aspects of habitat heterogeneity, given the existence of separate effects of heterogeneity in land cover, vegetation, and climate on species richness gradients (Stein, Gerstner, & Kreft, 2014; Tuanmu & Jetz, 2015). Land cover heterogeneity is a measurement of the number of unique habitats that can be distinguished based on differences in their vegetation type and structure, and was calculated using MODIS land cover classification. The standard deviation of productive and ambient energy measures provide both among and within-land cover measures of habitat heterogeneity, and were calculated from the energy and productivity measurements cited above.

4) Water limits species richness by limiting primary production. Annual precipitation was obtained from the GLDAS Noah Land Surface Model, and uses a combination of remote sensing and interpolated weather station data (Rodell & Beaudoing, 2013). Actual Evapotranspiration (AET) or the amount of water that is removed from a surface due to evaporation and transpiration was obtained from the NTSG (Mu et al., 2011). Both precipitation and AET are expected to correlate closely to productivity measures at broad scale.

5) Land cover change incorporates a direct component of human impact, by separating human-dominated landscapes (i.e. agricultural, pasture, urban) from a

diversity of natural landscapes. I identified the dominant land cover type within a quadrat, from the MODIS IGBP land cover classification scheme (Friedl et al., 2010), as a measure of both human impact and ecosystem function. Finally, global patterns of human appropriation of NPP (HANPP) reveal the combined effect of harvest and productivity changes induced by land use on the availability of NPP in ecosystems (Haberl, Erb, & Krausmann, 2014). Here, I used a concurrent dataset to HANPP, NPPt, as the amount of NPP remaining in ecosystems after harvest where HANPP = NPP_0 – NPPt, with NPP_0 being the plant cover that would prevail in the absence of human intervention (Haberl et al., 2007). Although HANPP datasets are not obtained solely through remote sensing, these were included in the study as a potential complement to NPP measurements.

There is strong collinearity among many of the environmental metrics included here. To explore patterns of multicollinearity in detail and to identify independent factors that explain the maximum amount of mutual correlation, I performed a principal component analysis (PCA). The first three principal components separated into orthogonal axes of productive energy, heat energy, and habitat heterogeneity (Table B1). I subsequently ran three separate PCAs for each of the three main groups of variables to identify a single metric from the larger set of variables. The selection was based on the variable having the highest correlation with the principal component (Table 2). The cumulative proportion represents the proportion of variability explained by consecutive principal components, and was used to determine the number of variables necessary to retain an acceptable level of variance. The first principal components for productive energy and heat energy accounted for 83.2% and 86.7% of the total variation among

those groups of variables, respectively, with mean annual EVI (EVI-mean) and mean annual PET measurements having the highest correlation coefficient with the respective components (98.7% and 98.8%, Table 2). Mean annual LST (LST-mean) correlates nearly as strongly to the first principal component as PET, with a correlation coefficient of 98.3%, and because PET is not measured in the most northerly environments, I used LST-mean instead. The PCA on habitat heterogeneity variables identified three principal components that accounted for 77.6% of the total variation: the standard deviation of EVI (EVI-SD), the standard deviation of LST (LST-SD), and land cover variety (LC-variety) were the three variables that correlated most strongly to the respective components. A single measurement of habitat heterogeneity from these variables was created using the first principal component of a PCA.

Data analysis

I plotted species richness with each remote sensing environmental variable[5] and constructed OLS regression models to explore relationships between species richness of birds and mammals, respectively, with each environmental variable at three spatial resolutions (100 km, 200 km, and 400 km). I square root-transformed species richness values to linearize its relationship with environmental predictors. Various combinations of EVI-mean, LST-mean, DHI-var, EVI-SD, LST-SD, LC-variety, and land cover type were tested and interaction terms were included. To allow non-linear relationships, quadratic terms for LST and DHI-var were also included. I used the Akaike Information Criterion (AIC) to compare models. AIC is a widely used information theory technique for model selection that estimates relative information content of a set of models. The

[5] See Appendix A, Figure A6, for examples

best model has the lowest AIC value, which suggests stronger evidence for that model over others. Models that are within 2 AIC values of the best model ($\Delta AIC < 2$) are also considered to have substantial support (Burnham & Anderson, 2004). My model building strategy relied on a set of pre-defined biological hypotheses that may be useful for application to global biodiversity monitoring. I favoured models containing fewer variables in instances where $\Delta AIC < 2$, and when the addition of the variable did not improve model pseudo R^2 by more than 1%. GLS models were fitted using maximum likelihood (or ML) and coefficients of determination (i.e. R^2) were not calculable or readily interpretable. I calculated pseudo R^2 values (calculated as the square of Pearson's correlation of observed and predicted y values) for models that AIC suggested were most informative.

The presence of spatial autocorrelation can bias estimates of the significance of a regression and the variables included. Methods that test for spatial autocorrelation in the error term generally produce more reliable model results than ordinary least squares (Beale, Lennon, Yearsley, Brewer, & Elston, 2010). Given the strong expectation of spatial autocorrelation in these models, I used generalized least squares (GLS), fitted with ML and an exponential correlation structure, to re-evaluate the fit of the models, as they perform consistently better than other methods when dealing with spatially autocorrelated data (Beale et al., 2010; Beguería & Pueyo, 2009; Dormann et al., 2007). I constructed a semivariogram of residuals to model the spatial covariance structure, a method often used with spatial GLS models that accounts for spatial autocorrelation at all distance lags, therefore requiring fewer initial assumptions compared to other spatial methods (Cressie, 1992; Dormann et al., 2007). High computational requirements required parallel

computing for constructing models at 100 km grid size. I ran 100 instances of each model and averaged AIC and pseudo R^2 values, using 20% of the observations. To evaluate the robustness of the results, I also ran simultaneous autoregressive models (SAR) using connectivity matrices from geographic coordinates of the center of grid cells with a threshold distance of 2000 km (Kissling & Carl, 2008). All statistical analyses were performed in the software R (*R Core Team*, 2017) , using the packages *nlme* to construct GLS models, *spdep* for SAR models, and *parallel* for computations in parallel.

I tested if large-scale trends inferred from models parameterized from areas with similar environmental characteristics are accurate, as such areas could be used to infer species richness trends in environmentally comparable areas where information on biodiversity is lacking or is difficult to obtain. To determine which regions to group together, I calculated the residual species richness from the global model for each biogeographical realm of the world, based on the most recent map of zoogeographic boundaries (Holt et al., 2013). Therefore, two groups were formed including tropical realms (i.e. Afrotropical, Neotropical, and Oriental) and non-tropical realms (i.e. Australian, Nearctic, Palearctic, Saraho-Arabian, and Sino-Japanese) and used to predict species richness of realms within the group (Figure B1). Predictions from models fitted using cross-validation were compared to predictions of within-realm models.

Mapping prediction thresholds

Maps of the limits to predictions were based on maximum observed values within each realm for each predictor variable included in the best model (Figure 2B). I extracted the maximum observed EVI-mean, LST-mean and HAB.HET value within the realm, which was used as the upper limit of prediction. The distance of a quadrat to the upper

regional limit was obtained by calculating the difference between the quadrat environmental values to the upper limit. Values that are observed beyond the upper limit would necessitate extrapolation beyond environment-richness combinations observed anywhere within that distinct realm.

Results

Species richness patterns in birds displayed stronger relationships with remotely-sensed environmental metrics than mammals at all spatial scales (Table 3). The importance of EVI-mean, the first PC of habitat heterogeneity (HAB.HET), and the interaction between mean EVI-mean and HAB.HET were similar among scales and taxa.

At 400 km grid sizes, correlations between remote sensing metrics and global species richness values were strongest (pseudo $R^2_{birds} = 0.76$, $P < 0.001$; Pseudo $R^2_{mammals} = 0.68$, $P < 0.001$), and weakened with diminishing scale. Strong positive relationships were observed with EVI-mean, HAB.HET, and LST-mean, and the interaction between EVI-mean and HAB.HET. The strength of statistical relationships with all environmental metric declined from 400km to 100km quadrats. LST-mean was not significantly related to species richness at 100 km for either taxon, nor with mammals at the 200 km grid size (Table 3). At all scales, adding LC-type to the model increased model pseudo R^2 slightly (1-2%) but also increased AIC values, so this predictor was excluded from the final model. Adding a polynomial term to LST-mean improved AIC values for birds and mammals at 400 km.

Spatial autocorrelation was detected at all spatial scales, although GLS models showed reduced residual spatial autocorrelation in comparison to OLS regressions (e.g.

Figure 1). The semivariogram shows increasing spatial dependency between pairs of observations as a function of decreasing distance separating them in OLS models. With GLS models, high semivariance indicates that, at different distances, pairs of observations have dissimilar values. Accounting for spatial autocorrelation in GLS models caused some predictor variables to become less important or to drop out of models. I also examined SAR models to evaluate whether results were method-dependent. While the effect sizes of individual variables were usually consistent, pseudo R^2 values were higher in SAR models.

Differences in species richness were observed between biogeographical realms after accounting for environmental correlates. In all models, residual species richness was consistently higher than predicted by environmental metrics in the Afrotropics, Neotropics, and Oriental realms and lower in the Palearctic, Nearctic, Australian, Sino-Japanese, and Saharo-Arabian realms (400km quadrats; Figure B1). When species richness values of each realm were predicted by a model parameterized using data from environmentally similar realms, differences were observed between taxa and biogeographical realms and model predictions were weaker than models constructed from within-realm observations at 400 km ($R^2_{\text{cross-validation}}$ = 0.03-0.80, $R^2_{\text{within-realm}}$ = 0.21-0.88, Table B2). Cross-validation performed more poorly for mammals than birds, especially in the Afrotropical, Neotropical, Oriental, Nearctic, and Saharo-Arabian realms (R^2_{birds}= 0.05-0.80, R^2_{mammals}= 0.03-0.73). Within-realm models made strong predictions of species richness of birds, particularly in non-tropical realms ($R^2_{\text{non-tropical}}$ = 0.69-0.82).

Areas that are closest to their upper regional limit of prediction differ for each environmental metric. For EVI-mean values, it includes most of the Oriental realm, large

parts of the Amazonian region, Central Africa, and South-eastern Nearctic (Figure 3). For LST-mean values, those areas are spread in most of the Neotropics, the Saharo-Arabian and Australian realms, and in parts of the Oriental and Sino-Japanese realms. In comparison, close proximity to upper regional limit of prediction based on HAB.HET values can be found in more localized areas in the eastern Afrotropics, southern Palearctic, and western Nearctic.

Discussion

A core number of remotely-sensed EBVs explain gradients of diversity among birds and mammals within the zoogeographical realms of the world. These environmental metrics are consistently important across regions, scales, and between taxa. Existing and emerging remote sensing technologies are valuable for macroecological research and provide the means to monitor and to potentially predict changes in biodiversity. However, differences between biogeographical realms are persistent and likely reflect unique, and potentially historical, processes. As environmental conditions change, predictions for how species richness will respond will require extrapolation beyond the limits of present-day environmental conditions across significant areas of the world, and most particularly in areas that are characterized by high diversity and large numbers of range-restricted taxa (Zuloaga, Currie, & Kerr, in press).

Monitoring on-going change in environmental conditions

The importance of vegetation density and temperature, reflected by mean annual EVI and mean annual LST, are consistent with the species-energy relationship where areas that are typically warmer and most productive will harbor more diversity (Cusens,

Wright, McBride, & Gillman, 2012). However, remotely-sensed vegetation metrics like the EVI also reflect changes in habitat amount related to present-day anthropogenic changes attributed to land conversion, fragmentation and land-use intensity (Garbulsky & Paruelo, 2004; Hill & Donald, 2003; Kerr & Ostrovsky, 2003; Nagendra et al., 2013). Individual and potentially interactive effects of temperature and habitat loss on biological populations are expected to be dominant threats to biological diversity in the future (Hof, Araújo, Jetz, & Rahbek, 2011; Mantyka-pringle, Martin, & Rhodes, 2012; Mantyka-Pringle et al., 2015; Segan, Murray, & Watson, 2016). Alternatively, areas where resource availability increases due to global warming might experience an increase in diversity, and provide climatic and environmental refugia for an array of species (Berteaux et al., 2018). There is considerable value in demonstrating consistent, scalable links between readily-accessible remote sensing measurements that relate to those threats, and relationships identified here may be valuable for improving monitoring of biodiversity change and predicting those changes in the future.

Habitat heterogeneity (Table 3) is also strongly related to species richness among both mammals and birds (Kerr & Packer, 1997; Stein et al., 2014). Increased habitat heterogeneity enhances the diversity of resources and structural complexity, which can increase available niche space and thereby promote species' coexistence (Pereira, Alves da Silva, Alves, Matos, & Fonseca, 2012; Tscharntke et al., 2012). Extensive habitat loss and land conversion may have significant implications on avian and mammalian diversity. Land use changes and intensification reduces habitat heterogeneity, and leads to homogenization of biotic communities with potential consequences for ecosystem services also (Gossner et al., 2016; Schulte, Mladenoff, Crow, Merrick, & Cleland,

2007). The significant positive interaction term between habitat heterogeneity and EVI-mean shows a non-linear relationship between richness and productive energy and may indicate novel impacts of climate change in the near future. As observed previously by Kerr & Packer, (1997), an increase in available energy caused by global warming may increase the importance of habitat heterogeneity as a prime determinant of species richness patterns in some areas.

Predicting biodiversity

To mitigate future losses in biodiversity and improve potential for management interventions, models that reliably predict biodiversity decline are critical. My results demonstrate that within-realm models can predict spatial gradients of species richness accurately in many regions of the world, with some within-realm models explaining up to 88% of the variation in species richness of birds (Table B2). However, species richness within a region is far less well predicted by richness-environment relationships derived using data from other realms with comparable climate and richness estimates. Consistent with that conclusion, predictions in areas where environmental conditions go beyond those observed in the regions where data was parametrized often underestimated or overestimated observed richness (Figure 2). These results are consistent with previous studies demonstrating that, among terrestrial vertebrates, environment-richness models differ regionally (Qian, 2008, 2010). The influence of evolutionary history and faunal assemblages in shaping global-scale models weakens the expected relationship between important environmental drivers and species richness and limits predictions of biodiversity to remain within their respective realms.

Regional history also hinders our ability to predict the effect of future changes in areas where environmental conditions are expected to exceed or subceed those currently observed within that region. Although biodiversity estimates can be interpolated regionally and give us insight on large-scale changes, predictions in areas close to the upper environmental limit of prediction should be treated with even greater caution. If the magnitude of richness differed but the effect of environmental variables remained consistent across realms (i.e. if the slopes were stable across realms), predictions arising from novel environmental conditions can be expected to be in line with regional richness baselines. Given that environment-richness relationships vary by realm for birds and mammals, attempts to predict how diversity will respond to environmental changes that exceed conditions previously observed there are risky.

Areas where regional environmental limits imposes greater predictive caution includes an array of ecosystems including deserts, grasslands, temperate and tropical forests, while mostly occurring in low latitudes (Figure 3). However, efforts for monitoring biodiversity and ecological field work are particularly insufficient in those areas, creating additional uncertainty over predictions of future change. The lack of comprehensive biodiversity time series for large groups like mammals and birds make temporal comparisons challenging at the macroecological scale. However, the EBV framework and related initiatives (i.e. BON in a Box; GEO BON, 2018) are helping the acquisition of relevant biodiversity information that could improve the representativeness of global biodiversity datasets. The on-going production of core biodiversity metrics, including species distribution and population abundance, will form the basis of efficient and coordinated monitoring that will help fill that gap (Pereira et al., 2013). Likewise,

remote sensing EBVs will be important in generating scalable data that may play a key role in improving predictions of change at the macroecological scale. Most macroecological models that rely on the space-for-time assumption, have been tested for a limited group of taxa or do not reflect changes associated to human activity. New remote sensing data and biological data that capture rapid change in environmental conditions may be essential in the near future to build stronger, mechanistic theories in macroecology that can successfully predict biodiversity changes.

Limitations

Patterns arising at broad spatial scale differ from landscape processes, from which management decisions are generally made. Coarser grains have been found to be associated with stronger environment-richness (Belmaker & Jetz, 2015; Stein et al., 2014), whereas processes underlying fine-grained richness gradients are associated with processes such as competition and predation, or effects of regionals species pool and dispersal distance (Brown, Reilly, & Peet, 2016). Although results of this research is not directly translatable to conservation decision-making at a local scale, the scale at which the analysis was performed can help identify places where changes resulting from anthropogenic activities are expected to be more severe, and reassess allocation of conservation resources.

My conclusions were based on the distribution of all species of birds and terrestrial mammals for which data was available from the IUCN. However, by removing quadrats where land area is lesser than 50% of the area of the quadrat, many coastal areas were excluded from the analysis, along with species whose ranges stand exclusively in those areas. Therefore, the environment-richness relationships described in this study

may not reflect processes occurring in coastal areas. Given that coastal habitats are expected to undergo major changes, close biological and remote sensing monitoring will be necessary to understand and predict changes in these ecologically distinct and climatically vulnerable ecosystems.

Conclusion

Current trends of decline in biodiversity at the global scale requires operational monitoring systems that provide accurate information about changes in ecosystems at regional and global scales. By assembling biodiversity-relevant remote sensing metrics and applying widely recognized macroecological concepts, our research demonstrates that the consequences of climate change and habitat loss on global biodiversity gradients can be measured, potentially proving effective in predicting global change effects on species richness trends. This study also provides practical considerations to biodiversity monitoring, by highlighting specific areas where the uncertainty in biodiversity predictions demands enhanced monitoring efforts. Remote sensing can facilitate the delivery of metrics of ecosystem function and structure that are sensitive to change and that capture changes at multiples scales, proving valuable for many applications in biodiversity conservation. Given the inherent capacity of remotely-sensed metrics to accommodate multiple structures and at multiple scales, there is an opportunity to bridge biodiversity information with remote sensing metrics to further investigate macroecological patterns of biodiversity and contemporary underlying drivers.

Tables and Figures

Table 1 Statistics measured to evaluate relationship between avian and mammalian species richness to environmental variables, with corresponding information on product name, sensor and satellite, spatial (SR) and temporal resolution (TR), source and time period of acquired imagery.

Product	Name	Satellite and sensor	SR (km)	TR	Source	Time	Statistics
Dynamic Habitat Index (DHI)	MOD15A2 v5	MODIS: Terra, Aqua	1	8-day	SILVIS Lab (http://silvis.forest.wisc.edu/dhi)	2003-2010	TOT, MIN, temporal variation
Actual Evapotranspiration (AET)	MOD16 v55	MODIS: Terra, Aqua	1	Monthly	NTSG	2001-2010	TOT, MIN, MAX, SD
Enhanced Vegetation Index (EVI)	VIPPHEN EVI2	MODIS: Terra	~ 6	Yearly	USGS	2001-2010	MEAN, MIN, MAX, SD
Normalized Difference Vegetation Index (NDVI)	VIPPHEN NDVI	MODIS: Terra	~ 6	Yearly	USGS	2001-2010	MEAN, MIN, MAX, SD
Net Primary Productivity (NPP)	MOD17 v55	MODIS: Terra, Aqua	1	Yearly	NTSG	2001-2010	MEAN, SD
Gross Primary Productivity (GPP)	MOD17 v55	MODIS: Terra, Aqua	1	Yearly	NTSG	2001-2010	MEAN, SD
Human appropriation of Net Primary Productivity (HANPP)	Modelled	-	10	Single year	University of Klagenfurt (https://www.aau.at/blog/global-hanpp-2000/)	2000	MEAN, SD
Precipitation (PREC)	GLDAS-2	Various products	~ 28	Monthly	GES DISC	2001-2010	TOT
Potential Evapotranspiration (PET)	MOD16 v55	MODIS: Terra, Aqua	1	Monthly	NTSG	2001-2010	TOT, MIN, MAX, SD
Land Surface Temperature (LST)	MOD11C3 v6	MODIS: Terra	~ 6	Monthly	USGS	2001-2010	MEAN, MIN, MAX, SD
Land cover (LC)	MCD12C1 v51	MODIS: Terra, Aqua	~ 6	Yearly	USGS	2001-2010	Majority, Variety

SD = standard deviation, TOT = annual sum, MIN = annual minimum, MAX = annual maximum, MEAN = annual mean, USGS = US Geological Survey, NTSG = Numerical Terradynamic Simulation Group, GES DISC = Goddard Earth Sciences Data and Information Services Center

Table 2 First three principal components of the principal component analysis (PCA) performed on remotely-sensed environmental metrics. The cumulative proportion, a measure of the added proportion of variance explained by the principal components, was used to determine the number of variables to include. Other values indicate the correlation of each variable to the principal component. Variables with the highest value within each principal component for the three main groups (vegetation amount, heat-related energy, habitat heterogeneity) were used to construct models and are shown in green.

	PC1	PC2	PC3
Vegetation amount			
DHI-min	0.846	-0.448	0.167
DHI-tot	0.984	0.007	0.074
ET-tot	0.947	0.109	-0.241
ET-min	0.857	-0.079	-0.442
ET-max	0.881	0.368	-0.061
EVI-max	0.881	0.388	0.196
EVI-mean	**0.987**	-0.048	0.112
EVI-min	0.880	-0.442	0.076
GPP-mean	0.984	-0.012	-0.003
HANPP-mean	0.827	0.056	-0.191
NDVI-max	0.846	0.487	0.158
NDVI-mean	0.984	0.029	0.110
NDVI-min	0.902	-0.402	0.032
NPP-mean	0.925	0.078	-0.040
PREC-tot	0.929	-0.086	0.024
Cumulative proportion (%)	0.832	0.907	0.935
Heat-related energy			
PET-max	0.883	-0.419	-0.185
PET-min	0.926	0.339	-0.087
PET-tot	0.988	-0.012	-0.126
LST-max	0.883	-0.411	0.207
LST-mean	**0.983**	0.089	0.129
LST-min	0.918	0.374	0.064
Cumulative proportion (%)	0.867	0.969	0.989

Habitat heterogeneity			
LC-variety	-0.533	-0.255	**-0.642**
EVI-SD	**-0.880**	-0.104	-0.197
NDVI-SD	-0.843	0.007	-0.311
NPP-SD	-0.818	-0.389	0.124
GPP-SD	-0.834	-0.408	0.217
ET-SD	-0.826	-0.102	0.334
HANPP-SD	-0.647	-0.104	0.359
LST-SD	-0.617	**0.682**	-0.102
PET-SD	-0.456	0.661	0.311
Cumulative proportion (%)	0.508	0.677	0.776

Table 3 Performance of the Generalized Least Squares (GLS) model with the lowest AIC, explaining global avian and mammalian richness patterns from remote sensing metrics, at grain sizes of 100 km x 100km, 200 km x 200 km, and 400 km x 400 km. ***P < 0.001, **P < 0.01, *P < 0.1. (+) indicates that the factor variable was included in the best model whereas (–) indicates the variable (factor or continuous) was not. SE = standard error.

	100 km		**200 km**		**400 km**	
Variables	*Coefficient*	*(SE)*	*Coefficient*	*(SE)*	*Coefficient*	*(SE)*
Birds						
Mean EVI	9.726***	(0.446)	8.921***	(0.679)	12.218***	(1.733)
Mean LST, 2	-	-	-0.002***	(0.001)	-0.002***	(0.001)
Mean LST	-	-	0.030*	(0.008)	0.135***	(0.035)
HAB.HET	0.272***	(0.030)	0.410***	(0.043)	0.987***	(0.114)
HAB.HET*EVI	0.610***	(0.102)	1.040***	(0.154)	1.151**	(0.008)
LC	-		-		-	
Realm	-		-		+	
Pseudo R²	0.604		0.602		0.762	
Mammals						
Mean EVI	3.656***	(0.213)	3.936***	(0.307)	6.655***	(0.898)
Mean LST, 2	-	-	-	-	-0.001**	(0.000)
Mean LST	-	-	-	-	0.052*	(0.021)
HAB.HET	0.155***	(0.014)	0.246***	(0.023)	0.466***	(0.038)
HAB.HET*EVI	0.103	(0.049)	0.240**	(0.084)	-	-
LC	-		-		-	
Realm	-		-		+	
Pseudo R²	0.566		0.584		0.683	

Table 4 AIC values for Generalized least squares (GLS) models of avian and mammalian species richness globally from remotely-sensed environmental metrics. The two best models, based on lowest AIC, are presented for each quadrat size.

	100 km	**200 km**	**400 km**
Model	*AIC*	*AIC*	*AIC*
Birds			
EVI, HAB.HET	7589.666		
EVI, HAB.HET, EVI*HAB.HET	**7583.933**		
EVI, HAB.HET, LST2, EVI*HAB.HET		**9657.05**	
EVI, HAB.HET, LST2, Realm, EVI*HAB.HET		9664.79	**3065.35**
EVI, HAB.HET, LST2, Realm			3070.55
Mammals			
EVI, HAB.HET	3755.947		
EVI, HAB.HET, EVI*HAB.HET	**3741.255**	**4858.04**	
EVI, HAB.HET, Realm, EVI*HAB.HET		4857.56	
EVI, HAB.HET, LST2, EVI*HAB.HET			1981.98
EVI, HAB.HET, LST2, Realm			**1979.80**

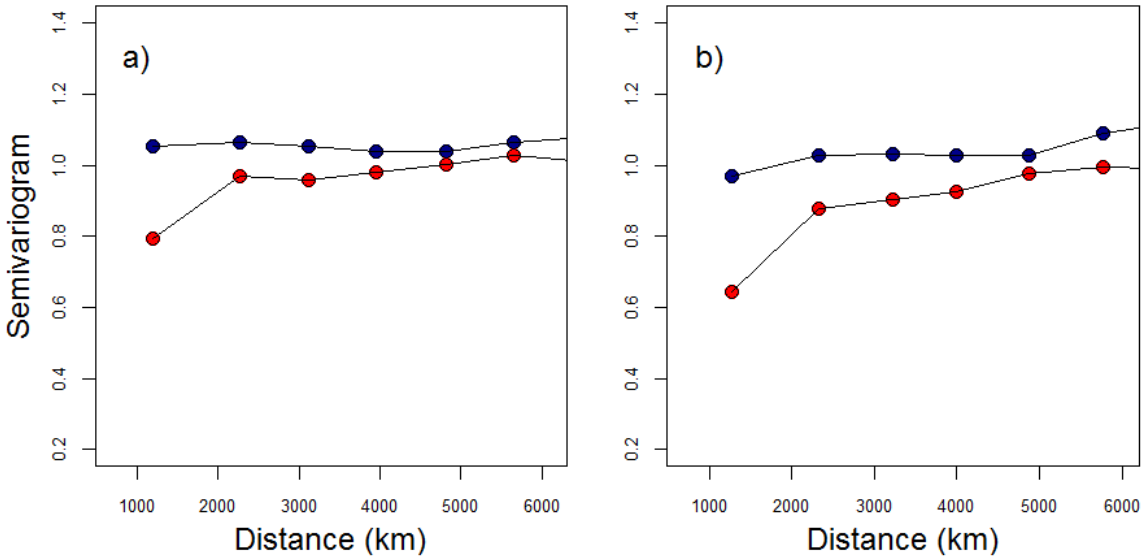

Figure 1 Semivariogram of residuals depicting spatial autocorrelation of sample points of the OLS model (red) and the GLS model (blue) for a) birds and b) mammals at 400 km grid size. Observations that are not spatially auto-correlated have high semi-variance values and vice-versa. With increasing distances, pairs of observations of OLS models show increasing semi-variance, denoting a decrease in spatial auto-correlation up to a certain distance, where semi-variance levels off. Pairs of observations from GLS regressions show stable semi-variance.

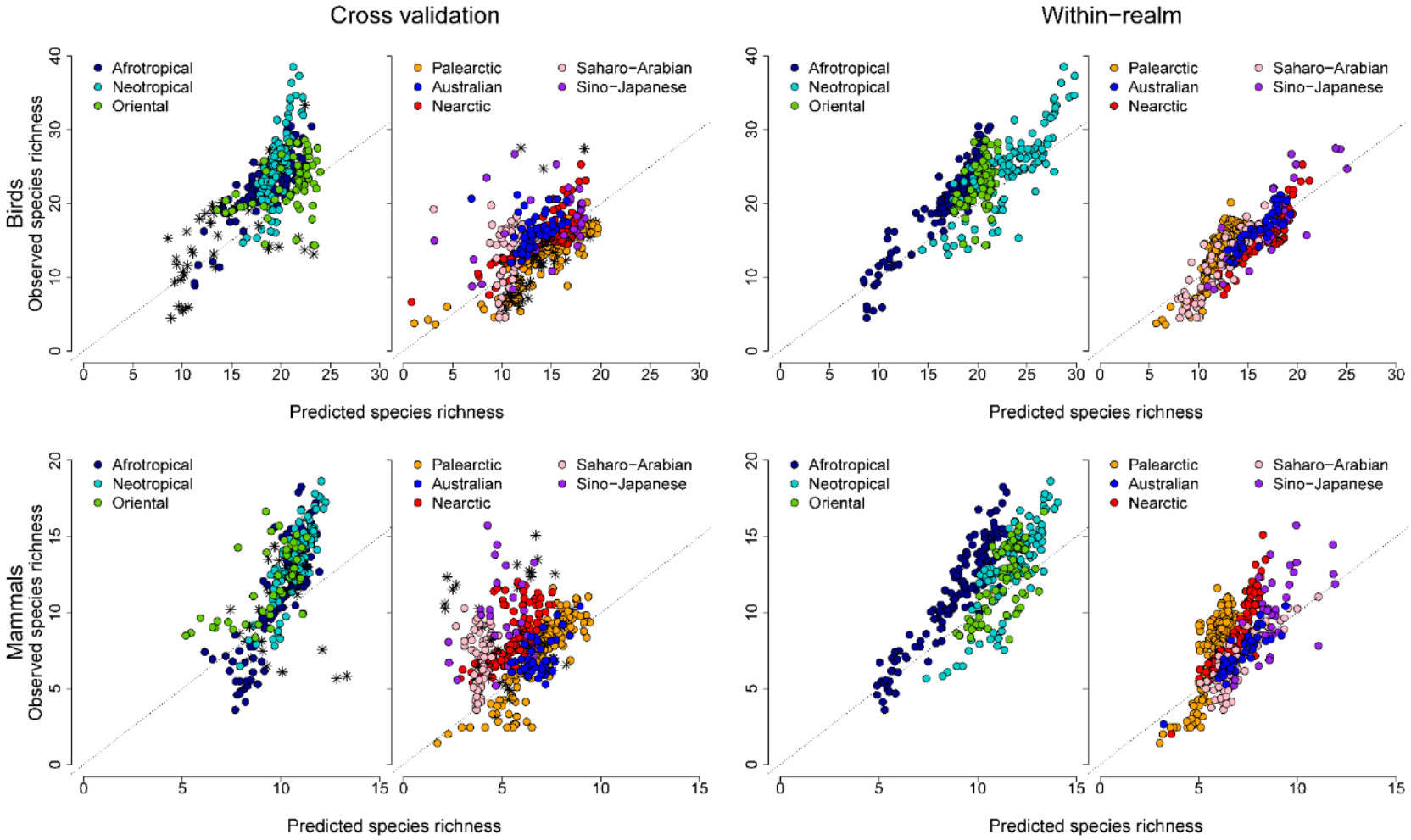
Cross validation
Within−realm
Birds
Mammals
Observed species richness
Predicted species richness
Afrotropical
Neotropical
Oriental
Palearctic
Australian
Nearctic
Saharo−Arabian
Sino−Japanese

Figure 2 Comparison of observed species richness of birds and mammals vs. predicted species richness using a model fitted from similar biogeographical realms (Cross-validation), and of observed species richness vs. predicted species richness using a model fitted to that same biogeographical realm (Within-realm), at 400 km grid size. The 1:1 reference line demonstrates perfect fit. Symbol * in cross validation panels shows quadrats where environmental conditions in the focus realm are not within the values used to parametrize the model, thus predictions are interpolated.

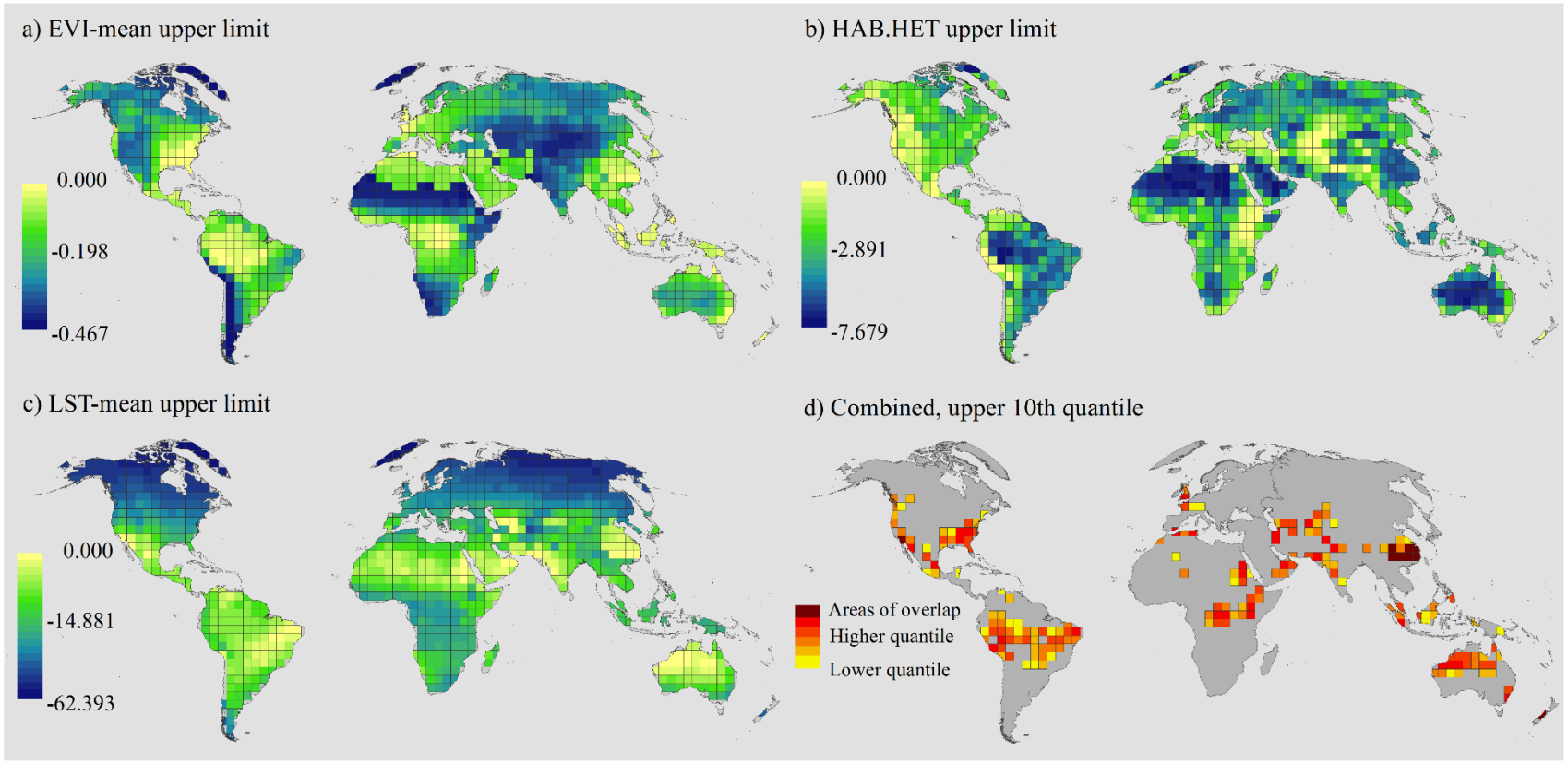

Figure 3 Distance of environmental conditions to their regional upper limit of prediction for three important remote sensing metrics including EVI-mean, habitat heterogeneity, LST-mean. Future change in areas closest to the upper threshold (close to 0) could create conditions where biodiversity responses are unpredictable. To show where such areas converge, the upper 10th quantile closest to the upper threshold of each metric was mapped (lower right panel), with areas close to the upper threshold of one environmental metric in

light blue, and areas close to the upper threshold of two or more of the environmental metrics in dark blue. All maps were projected to Goode homolosine equal area.

References

Algar, A. C., Kharouba, H. M., Young, E. R., & Kerr, J. T. (2009). Predicting the future of species diversity: macroecological theory, climate change, and direct tests of alternative forecasting methods. *Ecography*, *32*(1), 22–33. https://doi.org/10.1111/j.1600-0587.2009.05832.x

Beale, C. M., Lennon, J. J., Yearsley, J. M., Brewer, M. J., & Elston, D. A. (2010). Regression analysis of spatial data. *Ecology Letters*, *13*(2), 246–264. https://doi.org/10.1111/j.1461-0248.2009.01422.x

Beguería, S., & Pueyo, Y. (2009). A comparison of simultaneous autoregressive and generalized least squares models for dealing with spatial autocorrelation. *Global Ecology and Biogeography*, *18*(3), 273–279. https://doi.org/10.1111/j.1466-8238.2009.00446.x

Belmaker, J., & Jetz, W. (2015). Relative roles of ecological and energetic constraints, diversification rates and region history on global species richness gradients. *Ecology Letters*, *18*(6), 563–571. https://doi.org/10.1111/ele.12438

Berteaux, D., Ricard, M., St-Laurent, M.-H., Casajus, N., Périé, C., Beauregard, F., & de Blois, S. (2018). Northern protected areas will become important refuges for biodiversity tracking suitable climates. *Scientific Reports*, *8*(1). https://doi.org/10.1038/s41598-018-23050-w

BirdLife International and Handbook of the Birds of the World. (2016). Bird species distribution maps of the world. Version 6.0. Retrieved June 20, 2017, from http://datazone.birdlife.org/species/requestdis

Boucher-Lalonde, V., Kerr, J. T., & Currie, D. J. (2014). Does climate limit species richness by limiting individual species' ranges? *Proc. R. Soc. B*, *281*(1776), 20132695. https://doi.org/10.1098/rspb.2013.2695

Brown, R. L., Reilly, L. A. J., & Peet, R. K. (2016). Species Richness: Small Scale. In *eLS* (pp. 1–9). American Cancer Society. https://doi.org/10.1002/9780470015902.a0020488.pub2

Burnham, K. P., & Anderson, D. R. (2004). Multimodel Inference: Understanding AIC and BIC in Model Selection. *Sociological Methods & Research*, *33*(2), 261–304. https://doi.org/10.1177/0049124104268644

Butchart, S. H. M., Walpole, M., Collen, B., van Strien, A., Scharlemann, J. P. W., Almond, R. E. A., … Watson, R. (2010). Global Biodiversity: Indicators of Recent Declines. *Science*, *328*(5982), 1164–1168.

Collen, B., Loh, J., Whitmee, S., McRAE, L., Amin, R., & Baillie, J. E. M. (2009). Monitoring Change in Vertebrate Abundance: the Living Planet Index. *Conservation Biology*, *23*(2), 317–327. https://doi.org/10.1111/j.1523-1739.2008.01117.x

Connor, E. F., & McCoy, E. D. (1979). The Statistics and Biology of the Species-Area Relationship. *The American Naturalist*, *113*(6), 791–833.

Coops, N. C., Waring, R. H., & Landsberg, J. J. (1998). Assessing forest productivity in Australia and New Zealand using a physiologically-based model driven with averaged monthly weather data and satellite-derived estimates of canopy photosynthetic capacity. *Forest Ecology and Management*, *104*(1), 113–127. https://doi.org/10.1016/S0378-1127(97)00248-X

Coops, N. C., Waring, R. H., Wulder, M. A., Pidgeon, A. M., & Radeloff, V. C. (2009). Bird diversity: a predictable function of satellite-derived estimates of seasonal variation in canopy light absorbance across the United States. *Journal of Biogeography*, *36*(5), 905–918. https://doi.org/10.1111/j.1365-2699.2008.02053.x

Coops, N. C., Wulder, M. A., Duro, D. C., Han, T., & Berry, S. (2008). The development of a Canadian dynamic habitat index using multi-temporal satellite estimates of canopy light absorbance. *Ecological Indicators*, *8*(5), 754–766. https://doi.org/10.1016/j.ecolind.2008.01.007

Cressie, N. (1992). Statistics for Spatial Data. *Terra Nova*, *4*(5), 613–617. https://doi.org/10.1111/j.1365-3121.1992.tb00605.x

Currie, D. J. (1991). Energy and Large-Scale Patterns of Animal- and Plant-Species Richness. *The American Naturalist*, *137*(1), 27–49.

Currie, D. J., Mittelbach, G. G., Cornell, H. V., Field, R., Guégan, J.-F., Hawkins, B. A., … Turner, J. R. G. (2004). Predictions and tests of climate-based hypotheses of broad-scale variation in taxonomic richness. *Ecology Letters*, *7*(12), 1121–1134. https://doi.org/10.1111/j.1461-0248.2004.00671.x

Cusens, J., Wright, S. D., McBride, P. D., & Gillman, L. N. (2012). What is the form of the productivity–animal-species-richness relationship? A critical review and meta-analysis. *Ecology*, *93*(10), 2241–2252. https://doi.org/10.1890/11-1861.1

Didan, K. (2015). MOD13C2 MODIS/Terra Vegetation Indices Monthly L3 Global 0.05Deg CMG V006. *NASA EOSDIS LP DAAC*. https://doi.org/10.5067/MODIS/MOD13C2.006

Dormann, C. F., McPherson, J. M., Araújo, M. B., Bivand, R., Bolliger, J., Carl, G., … Wilson, R. (2007). Methods to Account for Spatial Autocorrelation in the Analysis of Species Distributional Data: A Review. *Ecography*, *30*(5), 609–628.

ESRI. (2016). (Version 10.4) [ArcGIS Desktop]. Redlands, CA. Environmental Systems Research Institute: ArcGIS Desktop.

Evans, K. L., James, N. A., & Gaston, K. J. (2006). Abundance, species richness and energy availability in the North American avifauna. *Global Ecology and Biogeography*, *15*(4), 372–385. https://doi.org/10.1111/j.1466-822X.2006.00228.x

Evans, K. L., Warren, P. H., & Gaston, K. J. (2005). Species-energy relationships at the macroecological scale: a review of the mechanisms. *Biological Reviews*, *80*(1), 1–25. https://doi.org/10.1017/S1464793104006517

Field, R., Hawkins, B. A., Cornell, H. V., Currie, D. J., Diniz-Filho, J. A. F., Guégan, J.-F., … Turner, J. R. G. (2009). Spatial species-richness gradients across scales: a meta-analysis. *Journal of Biogeography*, *36*(1), 132–147. https://doi.org/10.1111/j.1365-2699.2008.01963.x

Fjeldså, J., Bowie, R. C. K., & Rahbek, C. (2012). The Role of Mountain Ranges in the Diversification of Birds. *Annual Review of Ecology, Evolution, and Systematics*, *43*(1), 249–265. https://doi.org/10.1146/annurev-ecolsys-102710-145113

Friedl, M. A., Sulla-Menashe, D., Tan, B., Schneider, A., Ramankutty, N., Sibley, A., & Huang, X. (2010). MODIS Collection 5 global land cover: Algorithm refinements and characterization of new datasets. *Remote Sensing of Environment*, *114*(1), 168–182. https://doi.org/10.1016/j.rse.2009.08.016

Fritz, S. A., Eronen, J. T., Schnitzler, J., Hof, C., Janis, C. M., Mulch, A., … Graham, C. H. (2016). Twenty-million-year relationship between mammalian diversity and primary productivity. *Proceedings of the National Academy of Sciences of the United States of America*, *113*(39), 10908–10913. https://doi.org/10.1073/pnas.1602145113

Gámez-Virués, S., Perović, D. J., Gossner, M. M., Börschig, C., Blüthgen, N., de Jong, H., … Westphal, C. (2015). Landscape simplification filters species traits and drives biotic homogenization. *Nature Communications*, *6*. https://doi.org/10.1038/ncomms9568

Garbulsky, M. F., & Paruelo, J. M. (2004). Remote sensing of protected areas to derive baseline vegetation functioning characteristics. *Journal of Vegetation Science*, *15*(5), 711–720. https://doi.org/10.1111/j.1654-1103.2004.tb02313.x

GEO BON. (2018, January 17). BON in a Box. Retrieved July 25, 2018, from https://geobon.org/bon-in-a-box/

Gossner, M. M., Lewinsohn, T. M., Kahl, T., Grassein, F., Boch, S., Prati, D., … Allan, E. (2016). Land-use intensification causes multitrophic homogenization of grassland communities. *Nature; London*, *540*(7632), 266-269M. http://dx.doi.org.proxy.bib.uottawa.ca/10.1038/nature20575

Haberl, H., Erb, K. H., Krausmann, F., Gaube, V., Bondeau, A., Plutzar, C., … Fischer-Kowalski, M. (2007). Quantifying and Mapping the Human Appropriation of Net Primary Production in Earth's Terrestrial Ecosystems. *Proceedings of the National Academy of Sciences of the United States of America*, *104*(31), 12942–12947.

Haberl, H., Erb, K.-H., & Krausmann, F. (2014). Human Appropriation of Net Primary Production: Patterns, Trends, and Planetary Boundaries. *Annual Review of*

Environment and Resources, *39*, 363–391. https://doi.org/10.1146/annurev-environ-121912-094620

Hawkins, B. A., Field, R., Cornell, H. V., Currie, D. J., Guégan, J.-F., Kaufman, D. M., … Turner, J. R. G. (2003). Energy, Water, and Broad-Scale Geographic Patterns of Species Richness. *Ecology*, *84*(12), 3105–3117. https://doi.org/10.1890/03-8006

Hill, M. J., & Donald, G. E. (2003). Estimating spatio-temporal patterns of agricultural productivity in fragmented landscapes using AVHRR NDVI time series. *Remote Sensing of Environment*, *84*(3), 367–384. https://doi.org/10.1016/S0034-4257(02)00128-1

Hof, C., Araújo, M. B., Jetz, W., & Rahbek, C. (2011). Additive threats from pathogens, climate and land-use change for global amphibian diversity. *Nature*, *480*(7378), 516–519. https://doi.org/10.1038/nature10650

Holt, B. G., Lessard, J.-P., Borregaard, M. K., Fritz, S. A., Araújo, M. B., Dimitrov, D., … Rahbek, C. (2013). An Update of Wallace's Zoogeographic Regions of the World. *Science*, *339*(6115), 74–78. https://doi.org/10.1126/science.1228282

Honkanen, M., Roberge, J.-M., Rajasärkkä, A., & Mönkkönen, M. (2010). Disentangling the effects of area, energy and habitat heterogeneity on boreal forest bird species richness in protected areas. *Global Ecology and Biogeography*, *19*(1), 61–71. https://doi.org/10.1111/j.1466-8238.2009.00491.x

Huete, A., Didan, K., Miura, T., Rodriguez, E. P., Gao, X., & Ferreira, L. G. (2002). Overview of the radiometric and biophysical performance of the MODIS vegetation indices. *Remote Sensing of Environment*, *83*(1–2), 195–213. https://doi.org/10.1016/S0034-4257(02)00096-2

IUCN. (2016). The IUCN Red List of Threatened Species. Version 2016-1. Retrieved July 2, 2017, from http://www.iucnredlist.org

Jetz, W., & Fine, P. V. A. (2012). Global Gradients in Vertebrate Diversity Predicted by Historical Area-Productivity Dynamics and Contemporary Environment. *PLOS Biology*, *10*(3), e1001292. https://doi.org/10.1371/journal.pbio.1001292

Kadmon, R., & Allouche, O. (2007). Integrating the Effects of Area, Isolation, and Habitat Heterogeneity on Species Diversity: A Unification of Island Biogeography and Niche Theory. *The American Naturalist*, *170*(3), 443–454. https://doi.org/10.1086/519853

Kalmar, A., & Currie, D. J. (2007). A Unified Model of Avian Species Richness on Islands and Continents. *Ecology*, *88*(5), 1309–1321. https://doi.org/10.1890/06-1368

Kerr, J. T., Kharouba, H. M., & Currie, D. J. (2007). The Macroecological Contribution to Global Change Solutions. *Science*, *316*(5831), 1581–1584. https://doi.org/10.1126/science.1133267

Kerr, J. T., & Ostrovsky, M. (2003). From space to species: ecological applications for remote sensing. *Trends in Ecology & Evolution*, *18*(6), 299–305. https://doi.org/10.1016/S0169-5347(03)00071-5

Kerr, J. T., & Packer, L. (1997). Habitat heterogeneity as a determinant of mammal species richness in high-energy regions. *Nature; London*, *385*(6613), 252–254. http://dx.doi.org.proxy.bib.uottawa.ca/10.1038/385252a0

Kissling, W. D., & Carl, G. (2008). Spatial autocorrelation and the selection of simultaneous autoregressive models. *Global Ecology and Biogeography*, *17*(1), 59–71. https://doi.org/10.1111/j.1466-8238.2007.00334.x

Laliberté, E., & Tylianakis, J. M. (2010). Deforestation homogenizes tropical parasitoid–host networks. *Ecology*, *91*(6), 1740–1747. https://doi.org/10.1890/09-1328.1

Lewthwaite, J. M. M., Debinski, D. M., & Kerr, J. T. (2016). High community turnover and dispersal limitation relative to rapid climate change. *Global Ecology and Biogeography*, *26*(4), 459–471. https://doi.org/10.1111/geb.12553

Mantyka-Pringle, C. S., Martin, T. G., & Rhodes, J. R. (2012). Interactions between climate and habitat loss effects on biodiversity: a systematic review and meta-analysis. *Global Change Biology*, *18*(4), 1239–1252. https://doi.org/10.1111/j.1365-2486.2011.02593.x

Mantyka-Pringle, C. S., Visconti, P., Di Marco, M., Martin, T. G., Rondinini, C., & Rhodes, J. R. (2015). Climate change modifies risk of global biodiversity loss due to land-cover change. *Biological Conservation*, *187*, 103–111. https://doi.org/10.1016/j.biocon.2015.04.016

Mittelbach, G. G., Steiner, C. F., Scheiner, S. M., Gross, K. L., Reynolds, H. L., Waide, R. B., … Gough, L. (2001). What Is the Observed Relationship Between Species Richness and Productivity? *Ecology*, *82*(9), 2381–2396. https://doi.org/10.1890/0012-9658(2001)082[2381:WITORB]2.0.CO;2

Mu, Q., Zhao, M., & W Running, S. (2011). Improvements to a MODIS Global Terrestrial Evapotranspiration Algorithm. *Remote Sensing of Environment*, *115*, 1781-1800. [Accessed from http://www.ntsg.umt.edu/project/modis/mod16.php]. https://doi.org/10.1016/j.rse.2011.02.019

Nagendra, H., Lucas, R., Honrado, J. P., Jongman, R. H. G., Tarantino, C., Adamo, M., & Mairota, P. (2013). Remote sensing for conservation monitoring: Assessing protected areas, habitat extent, habitat condition, species diversity, and threats. *Ecological Indicators*, *33*(Complete), 45–59. https://doi.org/10.1016/j.ecolind.2012.09.014

Newbold, T. (2018). Future effects of climate and land-use change on terrestrial vertebrate community diversity under different scenarios. *Proc. R. Soc. B*, *285*(1881), 20180792. https://doi.org/10.1098/rspb.2018.0792

O'Connor, B., Secades, C., Penner, J., Sonnenschein, R., Skidmore, A., Burgess, N. D., & Hutton, J. M. (2015). Earth observation as a tool for tracking progress towards

the Aichi Biodiversity Targets. *Remote Sensing in Ecology and Conservation*, *1*(1), 19–28. https://doi.org/10.1002/rse2.4

Pereira, H. M., Belnap, J., Brummitt, N., Collen, B., Ding, H., Gonzalez-Espinosa, M., … Vieira, C. (2010). Global biodiversity monitoring. *Frontiers in Ecology and the Environment*, *8*(9), 459–460. https://doi.org/10.1890/10.WB.23

Pereira, H. M., Ferrier, S., Walters, M., Geller, G. N., Jongman, R. H. G., Scholes, R. J., … Wegmann, M. (2013). Essential Biodiversity Variables. *Science*, *339*(6117), 277–278. https://doi.org/10.1126/science.1229931

Pereira, H. M., Leadley, P. W., Proença, V., Alkemade, R., Scharlemann, J. P. W., Fernandez-Manjarrés, J. F., … Walpole, M. (2010). Scenarios for global biodiversity in the 21st century. *Science (New York, N.Y.)*, *330*(6010), 1496–1501. https://doi.org/10.1126/science.1196624

Pereira, H. M., Navarro, L. M., & Martins, I. S. (2012). Global Biodiversity Change: The Bad, the Good, and the Unknown. *Annual Review of Environment and Resources*, *37*(1), 25–50. https://doi.org/10.1146/annurev-environ-042911-093511

Pereira, P., Alves da Silva, A., Alves, J., Matos, M., & Fonseca, C. (2012). Coexistence of carnivores in a heterogeneous landscape: habitat selection and ecological niches. *Ecological Research*, *27*(4), 745–753. https://doi.org/10.1007/s11284-012-0949-1

Perović, D., Gámez-Virués, S., Börschig, C., Klein, A.-M., Krauss, J., Steckel, J., … Westphal, C. (2015). Configurational landscape heterogeneity shapes functional community composition of grassland butterflies. *Journal of Applied Ecology*, *52*(2), 505–513. https://doi.org/10.1111/1365-2664.12394

Pettorelli, N., Owen, H. J. F., & Duncan, C. (2016). How do we want Satellite Remote Sensing to support biodiversity conservation globally? *Methods in Ecology and Evolution*, *7*(6), 656–665. https://doi.org/10.1111/2041-210X.12545

Pettorelli, N., Ryan, S., Mueller, T., Bunnefeld, N., Jdrzejewska, B., Lima, M., & Kausrud, K. (2011). REVIEW The Normalized Difference Vegetation Index (NDVI): unforeseen successes in animal ecology. *Climate Research*, *46*(1), 15–27. https://doi.org/10.3354/cr00936

Pettorelli, N., Safi, K., & Turner, W. (2014). Satellite remote sensing, biodiversity research and conservation of the future. *Philosophical Transactions of the Royal Society B: Biological Sciences*, *369*(1643). https://doi.org/10.1098/rstb.2013.0190

Pettorelli, N., Wegmann, M., Skidmore, A., Mücher, S., Dawson, T. P., Fernandez, M., … Geller, G. N. (2016). Framing the concept of satellite remote sensing essential biodiversity variables: challenges and future directions. *Remote Sensing in Ecology and Conservation*, *2*(3), 122–131. https://doi.org/10.1002/rse2.15

Pimm, S. L., Jenkins, C. N., Abell, R., Brooks, T. M., Gittleman, J. L., Joppa, L. N., … Sexton, J. O. (2014). The biodiversity of species and their rates of extinction,

distribution, and protection. *Science*, *344*(6187), 1246752. https://doi.org/10.1126/science.1246752

Preston, F. W. (1962). The Canonical Distribution of Commonness and Rarity: Part I. *Ecology*, *43*(2), 185–215. https://doi.org/10.2307/1931976

Proença, V., Martin, L. J., Pereira, H. M., Fernandez, M., McRae, L., Belnap, J., … van Swaay, C. A. M. (2016). Global biodiversity monitoring: From data sources to Essential Biodiversity Variables. *Biological Conservation*. https://doi.org/10.1016/j.biocon.2016.07.014

Qian, H. (2008). Effects of historical and contemporary factors on global patterns in avian species richness. *Journal of Biogeography*, *35*(8), 1362–1373. https://doi.org/10.1111/j.1365-2699.2008.01901.x

Qian, H. (2010). Environment–richness relationships for mammals, birds, reptiles, and amphibians at global and regional scales. *Ecological Research*, *25*(3), 629–637. https://doi.org/10.1007/s11284-010-0695-1

Qian, H., & Ricklefs, R. E. (2008). Global concordance in diversity patterns of vascular plants and terrestrial vertebrates. *Ecology Letters*, *11*(6), 547–553. https://doi.org/10.1111/j.1461-0248.2008.01168.x

R Core Team. (2017). (Version 3.4). R Foundation for Statistical Computing. Vienna, Austria: A language and environment for statistical computing. Retrieved from http://www.R-project.org/

Rahbek, C., Gotelli, N. J., Colwell, R. K., Entsminger, G. L., Rangel, T. F. L. V. B., & Graves, G. R. (2007). Predicting Continental-Scale Patterns of Bird Species Richness with Spatially Explicit Models. *Proceedings: Biological Sciences*, *274*(1607), 165–174.

Rodell, M., & Beaudoing, H. K. (2013, December 1). GLDAS Noah Land Surface Model L4 3 hourly 0.25 x 0.25 degree Version 2.0, version 020. NASA/GSFC/HSL. Goddard Earth Sciences Data and Information Services Center (GES DISC). Greenbelt, Maryland, USA. Retrieved from doi:10.5067/342OHQM9AK6Q

Running, S. W., Nemani, R. R., Heinsch, F. A., Zhao, M., Reeves, M., & Hashimoto, H. (2004). A Continuous Satellite-Derived Measure of Global Terrestrial Primary Production. *BioScience*, *54*(6), 547–560. https://doi.org/10.1641/0006-3568(2004)054[0547:ACSMOG]2.0.CO;2

Schulte, L. A., Mladenoff, D. J., Crow, T. R., Merrick, L. C., & Cleland, D. T. (2007). Homogenization of northern U.S. Great Lakes forests due to land use. *Landscape Ecology*, *22*(7), 1089–1103. https://doi.org/10.1007/s10980-007-9095-5

Segan, D. B., Murray, K. A., & Watson, J. E. M. (2016). A global assessment of current and future biodiversity vulnerability to habitat loss–climate change interactions. *Global Ecology and Conservation*, *5*, 12–21. https://doi.org/10.1016/j.gecco.2015.11.002

Skidmore, A. K., Pettorelli, N., Coops, N. C., Geller, G. N., Hansen, M., Lucas, R., … Wegmann, M. (2015). Environmental science: Agree on biodiversity metrics to track from space. *Nature*, *523*(7561), 403–405. https://doi.org/10.1038/523403a

Stein, A., Gerstner, K., & Kreft, H. (2014). Environmental heterogeneity as a universal driver of species richness across taxa, biomes and spatial scales. *Ecology Letters*, *17*(7), 866–880. https://doi.org/10.1111/ele.12277

Tscharntke, T., Tylianakis, J. M., Rand, T. A., Didham, R. K., Fahrig, L., Batáry, P., … Westphal, C. (2012). Landscape moderation of biodiversity patterns and processes - eight hypotheses. *Biological Reviews*, *87*(3), 661–685. https://doi.org/10.1111/j.1469-185X.2011.00216.x

Tuanmu, M.-N., & Jetz, W. (2015). A global, remote sensing-based characterization of terrestrial habitat heterogeneity for biodiversity and ecosystem modelling. *Global Ecology and Biogeography*, *24*(11), 1329–1339. https://doi.org/10.1111/geb.12365

Turner, W., Rondinini, C., Pettorelli, N., Mora, B., Leidner, A. K., Szantoi, Z., … Woodcock, C. (2015). Free and open-access satellite data are key to biodiversity conservation. *Biological Conservation*, *182*, 173–176. https://doi.org/10.1016/j.biocon.2014.11.048

Wan, Z., Hook, S., & Hulley, G. (2015). MOD11C3 MODIS/Terra Land Surface Temperature/Emissivity Monthly L3 Global 0.05Deg CMG V006. *NASA EOSDIS LP DAAC*. https://doi.org/10.5067/MODIS/MOD11C3.006

Whittaker, R. J., Nogués-Bravo, D., & Araújo, M. B. (2007). Geographical gradients of species richness: a test of the water-energy conjecture of Hawkins et al. (2003) using European data for five taxa. *Global Ecology and Biogeography*, *16*(1), 76–89. https://doi.org/10.1111/j.1466-8238.2006.00268.x

Wright, D. H. (1983). Species-Energy Theory: An Extension of Species-Area Theory. *Oikos*, *41*(3), 496–506. https://doi.org/10.2307/3544109

Zhao, M., Heinsch, F. A., Nemani, R. R., & Running, S. W. (2005). Improvements of the MODIS terrestrial gross and net primary production global data set. *Remote Sensing of Environment*, *95*(2), 164–176. https://doi.org/10.1016/j.rse.2004.12.011

Zuloaga, J., Currie, D. J., & Kerr, J. T. (in press). The origins and maintenance of global species endemism. *Global Ecology and Biogeography*.

Appendix A: Supplemental Methods

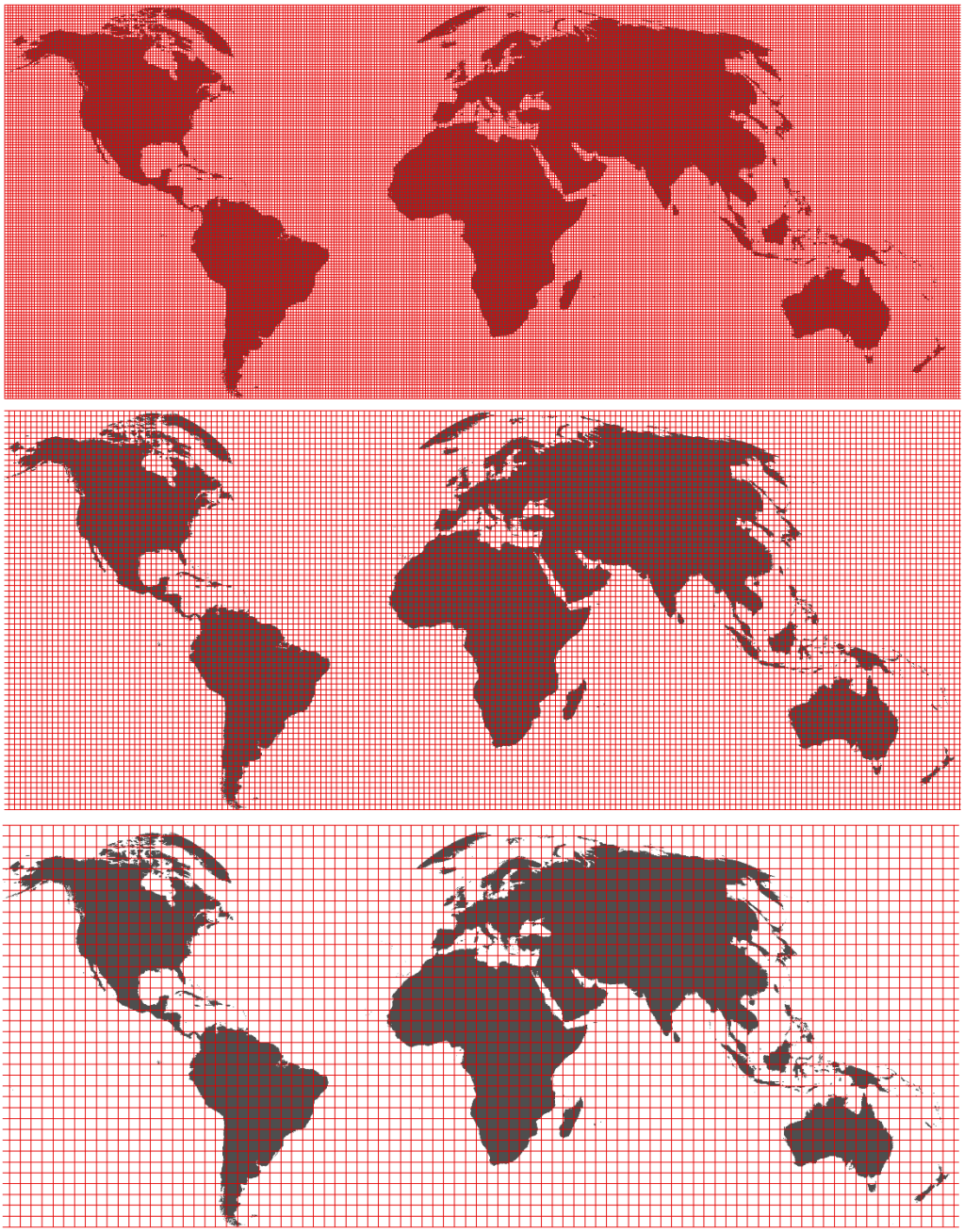

Figure A1 Quadrat system for aggregating environmental data and calculating species richness values, consisting of 100 km x 100 km grids (top), 200 km x 200 km grids (middle), and 400 km x 400 km grids (bottom).

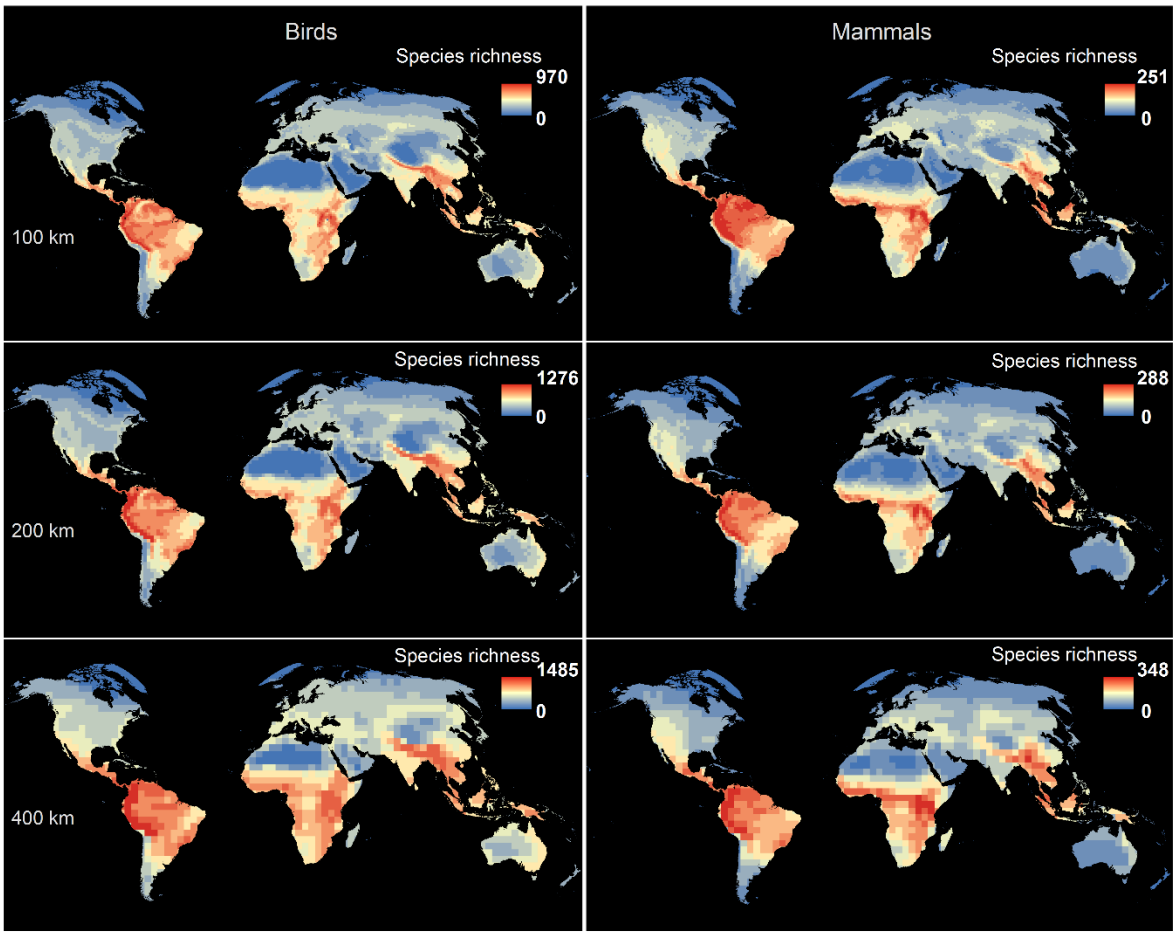

Figure A2 Species richness of birds and terrestrial mammals at 100 km, 200 km, and 400 km grid sizes. All maps were projected to Goode homolosine equal area.

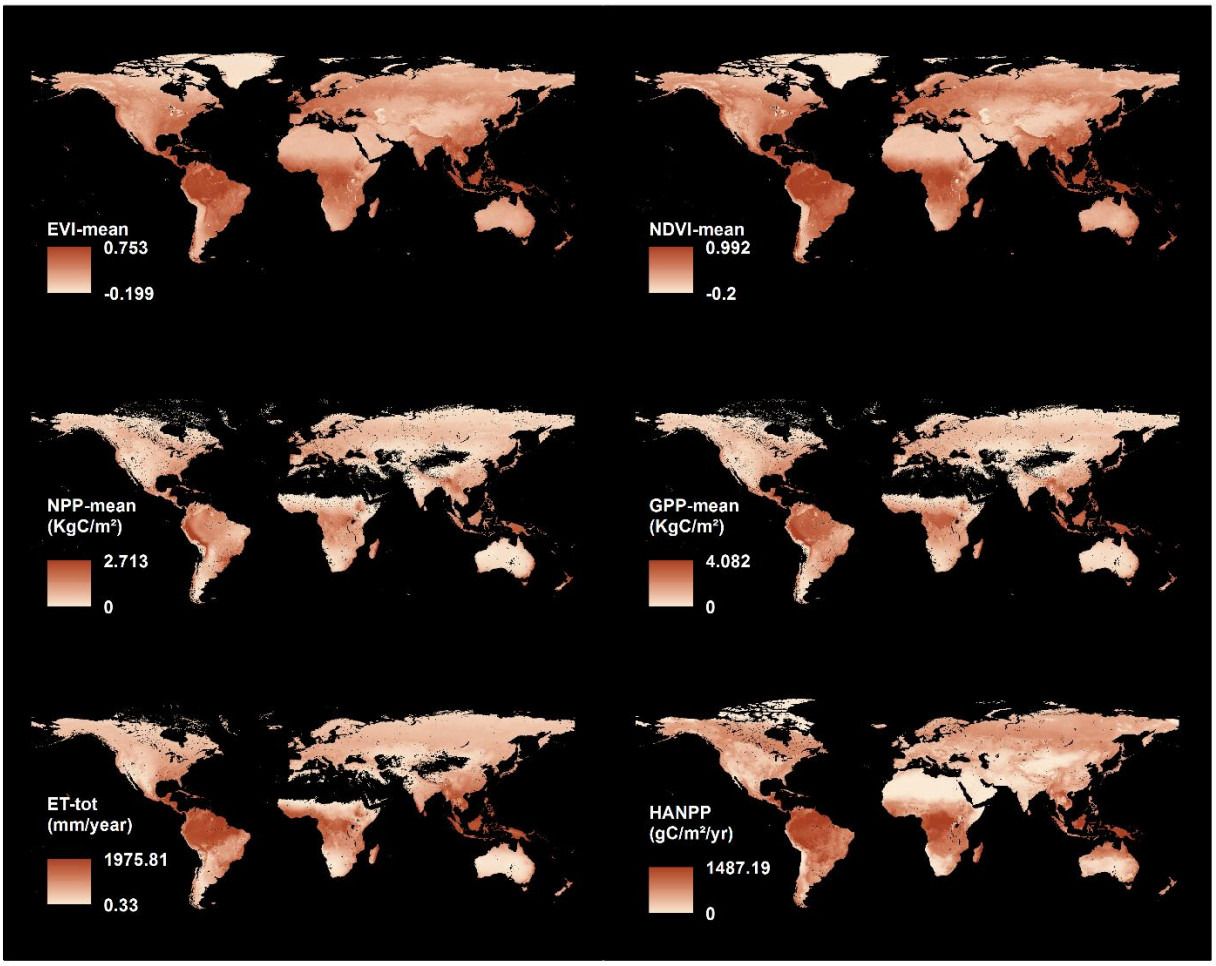

Figure A3 Remote sensing datasets related to vegetation amount, including mean annual Enhanced Vegetation Index (EVI), mean annual Normalized Difference Vegetation Index (NDVI), mean annual Net Primary Productivity (NPP), mean annual Gross Primary Productivity (GPP), total yearly Evapotranspiration (ET), and the Human Appropriation of NPP (HANPP), expressed as the NPP remaining in ecosystems after harvest. Minimum annual and maximum annual values were also calculated but are not shown. Annual values were averaged over the 2001-2010 period, except for the HANPP dataset for which only the year 2002 was available.

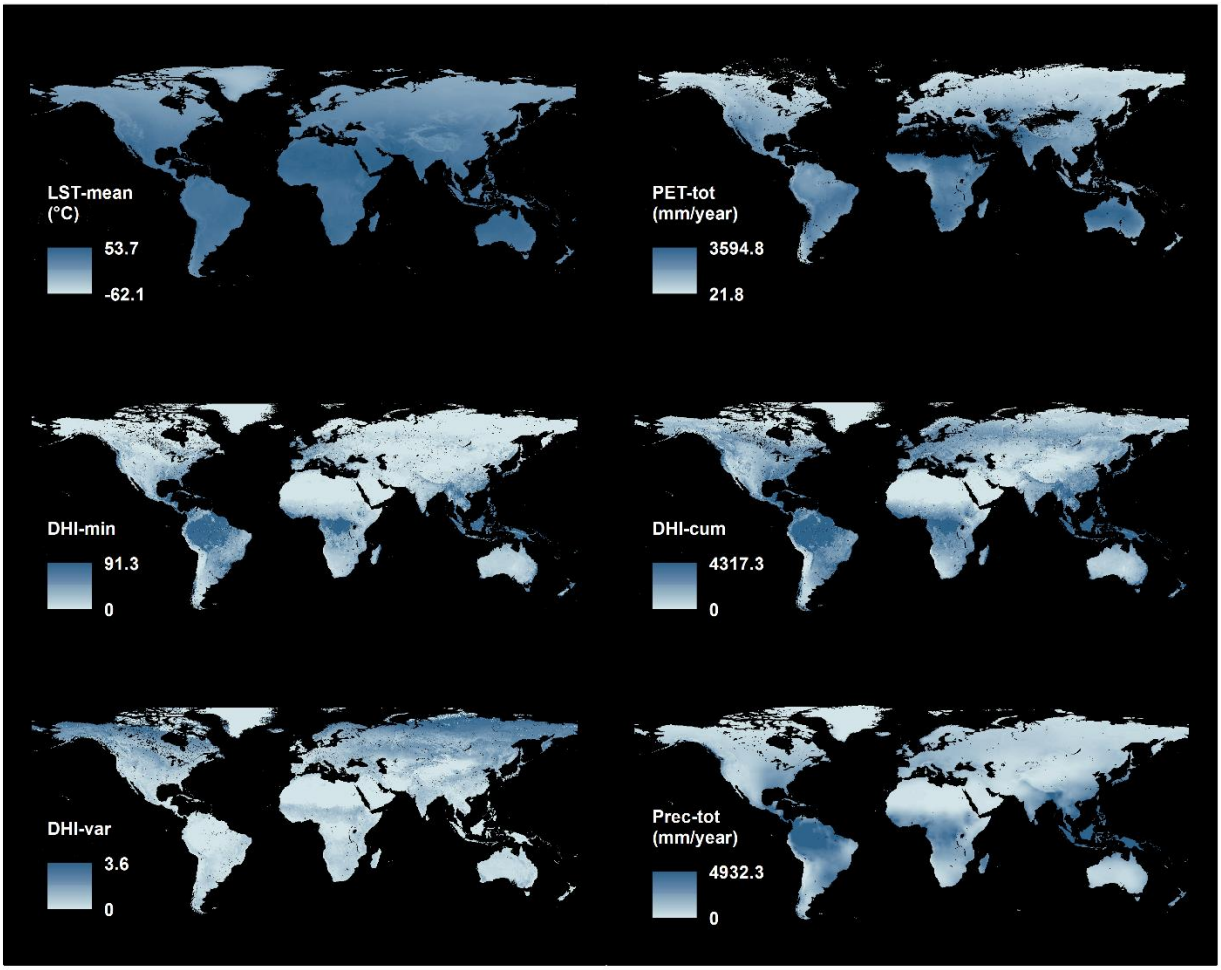

Figure A4 Remote sensing datasets related to vegetation amount and heat-related energy, including mean annual Land Surface Temperature (LST), mean annual Potential Evapotranspiration (PET), mean annual minimum Dynamic Vegetation Index (DHI), annual cumulative DHI, annual temporal variation in DHI, and precipitation. Minimum annual and maximum annual values were also calculated for LST and PET but are not shown. Annual values were averaged over the 2001-2010 period, except for the DHI datasets, which were averaged over the 2003-2010 period.

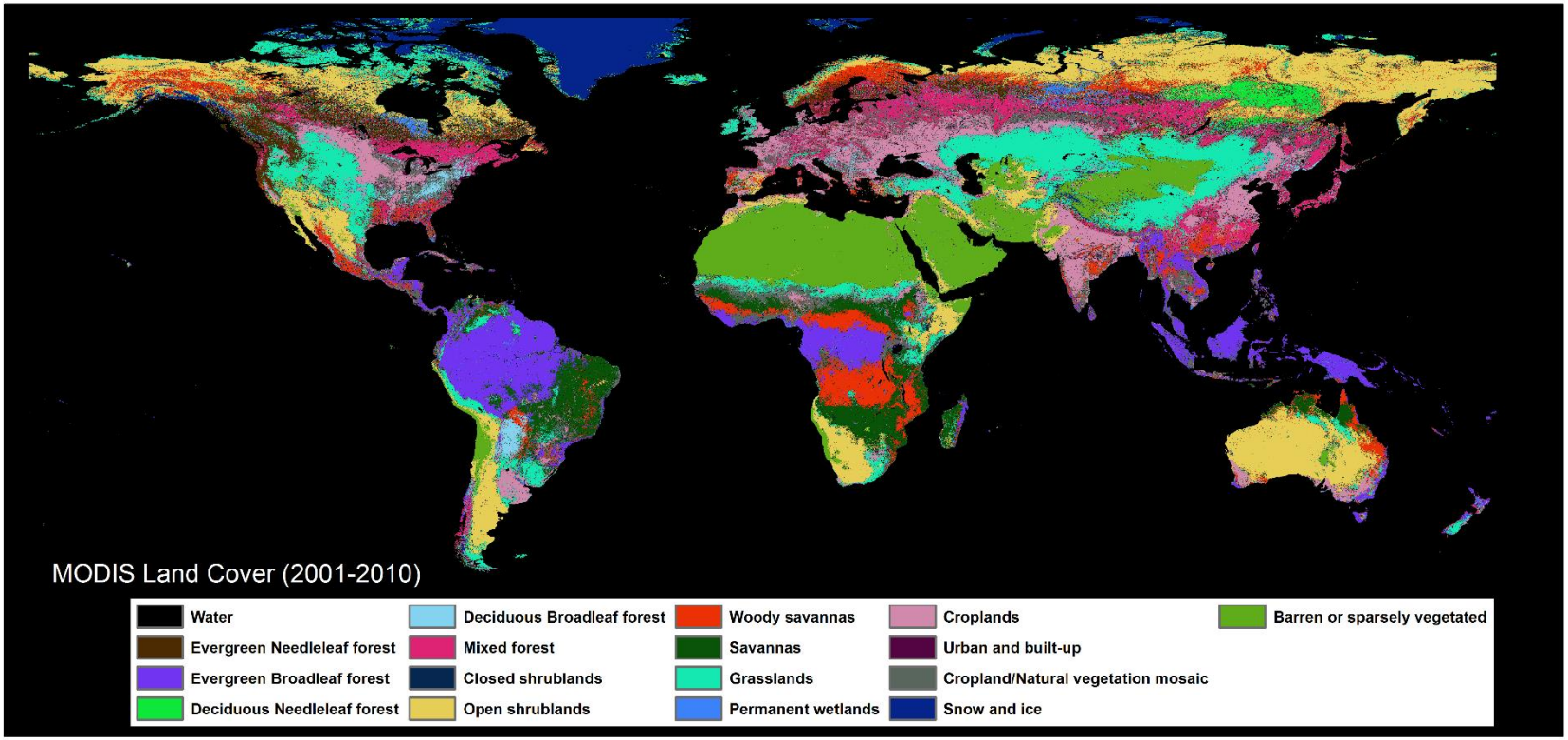

Figure A5 MODIS Land cover product (MCD12Q1) at 500 m resolution. For each cell, a single value was given according to the land cover type occurring most often between the 2001-2010 period (Majority statistic).

Table A1 List of acronyms and abbreviations

Abbreviation	Description
AET	Actual evapotranspiration
AIC	Akaike information criterion
DHI	Dynamic habitat index
DHI-cum	Cumulative Dynamic habitat index
DHI-min	Minimum Dynamic habitat index
DHI-var	Variance of Dynamic habitat index
EBV	Essential Biodiversity Variables
EVI	Enhanced vegetation index
GBIF	Global Biodiversity Information Facility
GES DISC	Goddard Earth Sciences Data and Information Services Center
GLDAS	Global Land Data Assimilation Systems
GLS	Generalized least lquares
GPP	Gross primary productivity
HAB.HET	Habitat heterogeneity
HANPP	Human appropriation of NPP
IGBP	International Geosphere-Biosphere Program
IUCN	International Union for Conservation of Nature
LC	Land cover
LST	Land surface temperature
MAX	Annual maximum
MIN	Annual minimum
ML	Maximum likelihood
MODIS	Moderate Resolution Imaging Spectroradiometer
NDVI	Normalized difference vegetation index
NPP	Net primary productivity
NTSG	Numerical Terradynamic Simulation Group
PCA	Principal component analysis
PET	Potential evapotranspiration
SAR	Simultaneous autoregressive
SD	Standard deviation
SR	Spatial resolution
TOT	Annual sum
TR	Temporal resolution
USGS	US Geological Survey

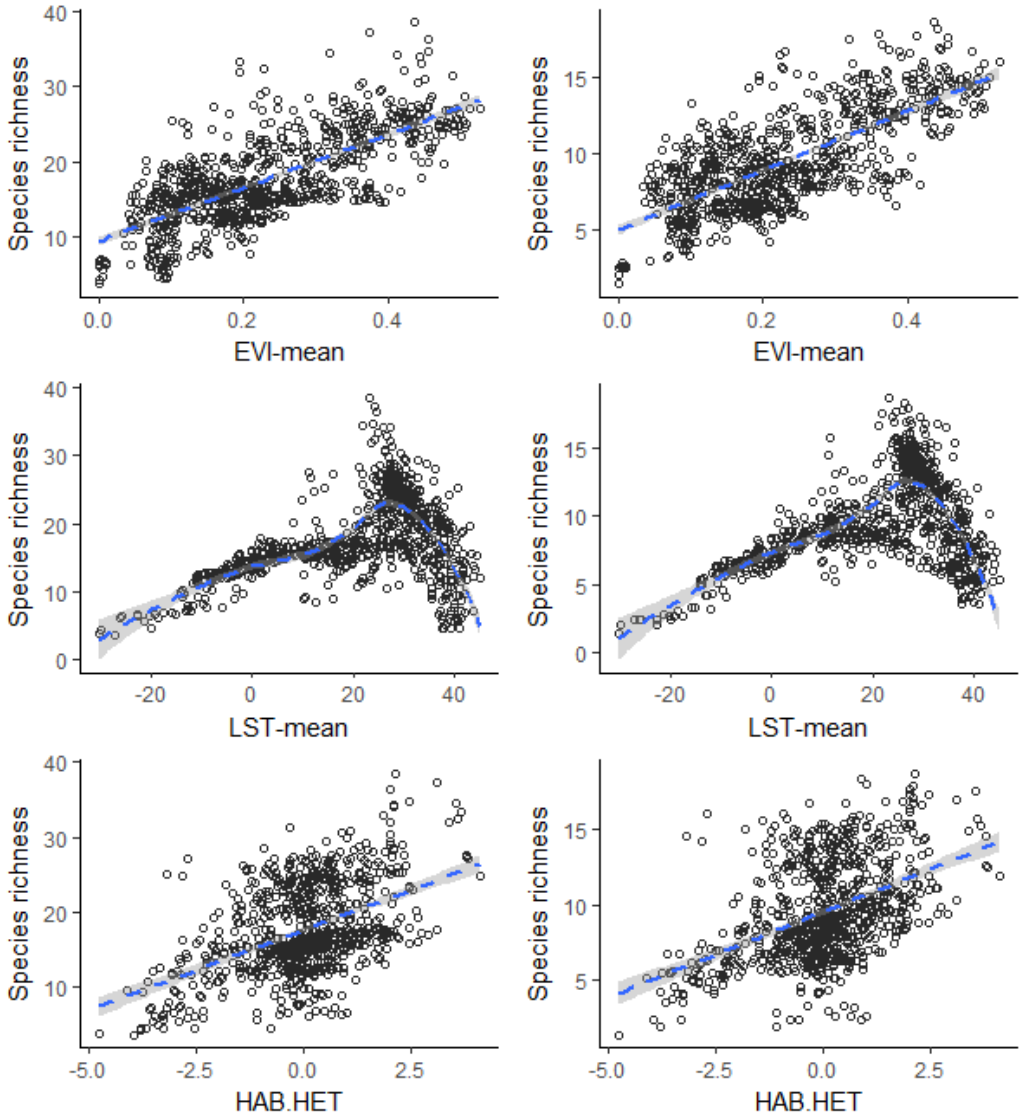

Figure A6. Scatterplot of species richness response to changing mean annual EVI, mean annual LST, and habitat heterogeneity at 400 km grid size for birds (left) and mammals (right).

Appendix B: Supplemental Results

Table B1 Principal Component Analysis (PCA) including all 31 variables and their correlation to the principal component.

Environmental variables	PC1	PC2	PC3	PC4	PC5
DHI-tot	0.95003	0.153244	-0.18409	0.026166	-0.00135
DHI-min	0.93981	-0.10682	-0.15206	-0.14727	-0.11838
DHI-var	-0.51019	0.694531	-0.05717	0.187863	0.241125
ET-max	0.82641	0.379726	-0.10804	0.114908	0.169245
ET-min	0.83901	0.012749	-0.09855	-0.36598	-0.07992
ET-SD	0.591303	-0.07781	0.59068	0.164695	0.105723
ET-tot	0.94046	0.124605	-0.08778	-0.1492	0.021485
EVI-max	0.80212	0.381025	-0.18972	0.231662	0.25002
EVI-mean	0.96504	0.04747	-0.17249	0.05449	0.06421
EVI-min	0.91877	-0.2917	-0.11845	-0.07082	-0.08492
EVI-SD	0.419258	0.210756	0.75878	0.035582	-0.10539
GPP-mean	0.96783	0.06069	-0.12653	-0.08181	-0.06276
GPP-SD	0.736959	0.086642	0.53976	0.118164	-0.19098
HANPP-mean	0.79751	0.129863	-0.23155	-0.09495	0.075132
HANPP-SD	0.50772	0.010336	0.40396	0.133996	0.295373
LST-max	-0.10738	-0.9166	0.010073	0.227682	0.009049
LST-mean	0.347177	-0.9105	0.020446	0.142794	0.02478
LST-min	0.542705	-0.7985	0.02462	0.092665	0.041829
LST-SD	-0.02762	-0.19587	0.73545	-0.37513	0.117714
NDVI-max	0.712583	0.547372	-0.19391	0.253667	0.217396
NDVI-mean	0.95392	0.143088	-0.16846	0.081769	0.044332
NDVI-min	0.93972	-0.23835	-0.11153	-0.08215	-0.09362
NDVI-SD	0.226252	0.203326	0.81853	0.128904	-0.10468
NPP-mean	0.90294	0.15706	-0.02408	-0.02623	-0.136
NPP-SD	0.619573	0.153383	0.57937	0.121781	-0.26092
PET-max	-0.07621	-0.9061	0.044306	0.243555	0.007215
PET-min	0.404768	-0.8045	-0.02724	0.06992	0.15722
PET-SD	0.002609	-0.33523	0.51636	-0.48382	0.456248
PET-tot	0.216811	-0.9481	0.019318	0.149219	0.054088
PREC-tot	0.89024	-0.01748	-0.1575	-0.14467	0.02589
LC-variety	0.083214	0.589161	0.46554	0.188196	0.049369
Standard deviation	3.8249	2.5742	1.938	1.03591	0.8648
Proportion of Variance	0.4719	0.2138	0.1212	0.03462	0.02412
Cumulative Proportion	0.4719	0.6857	0.8068	0.84147	0.86559

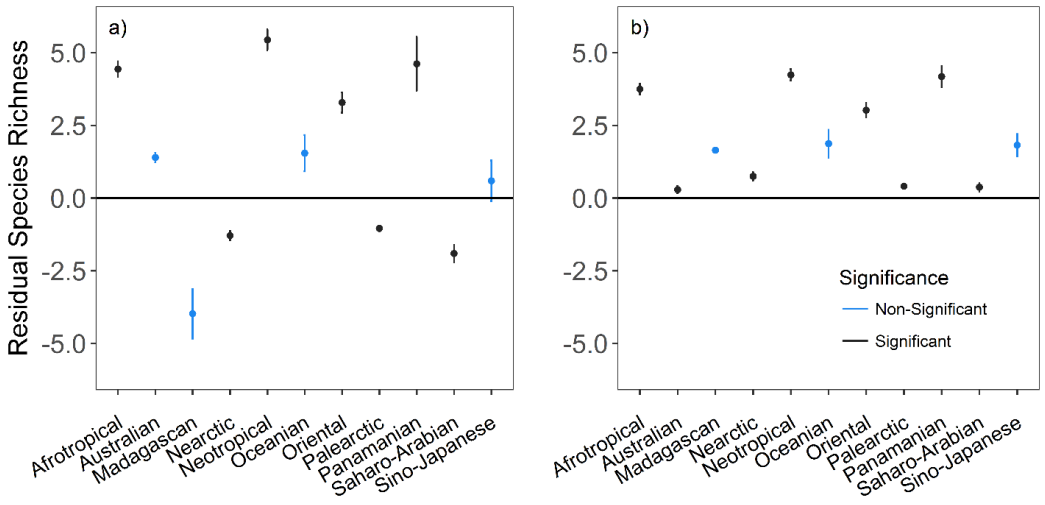

Figure B1 Residual species richness and standard error by zoogeographic realm at 400 km for a) birds and b) mammals. Black indicates significant difference in residual species richness from the global model (y = 0), and Blue indicates a non-significant difference. Significance threshold is $p < 0.01$. There are 11 distinct realms in this figure, but only 8 were used for cross-validations. Panamanian realm was merged to Neotropical realm, Madagascan and Oceanian realms were added to Oriental realm because they had too few quadrats to construct models from.

Table B2 Pseudo R^2 of generalized least squares (GLS) models of species richness on EVI-mean, LST-mean, HAB.HET, and a HAB.HET*EVI-mean interaction from cross-validated models and within-realm models. Cross-validation of models in Afrotropical. Neotropical, and Oriental realms were parametrized using data from the other two congruent realms. The same concept was applied to cross-validate models for Palearctic, Australian, Nearctic, Saharo-Arabian, and Sino-Japanese realms.

	Afrotropical	*Neotropical*	*Oriental*	*Palearctic*	*Australian*	*Nearctic*	*Saharo-Arabian*	*Sino-Japanese*
Cross validation								
Birds	0.801	0.276	0.124	0.783	0.098	0.685	0.054	0.102
Mammals	0.714	0.305	0.412	0.669	0.344	0.420	0.048	0.033
Within-realm								
Birds	0.881	0.667	0.217	0.797	0.783	0.817	0.780	0.689
Mammals	0.867	0.678	0.451	0.648	0.817	0.700	0.712	0.375